

Engineering Applications of Computational Fluid Mechanics

ISSN: 1994-2060 (Print) 1997-003X (Online) Journal homepage: <https://www.tandfonline.com/loi/tcfm20>

Comparative analysis of soft computing techniques RBF, MLP, and ANFIS with MLR and MNLR for predicting grade-control scour hole geometry

Hossien Riahi-Madvar, Majid Dehghani, Akram Seifi, Ely Salwana, Shahaboddin Shamsirband, Amir Mosavi & Kwok-wing Chau

To cite this article: Hossien Riahi-Madvar, Majid Dehghani, Akram Seifi, Ely Salwana, Shahaboddin Shamsirband, Amir Mosavi & Kwok-wing Chau (2019) Comparative analysis of soft computing techniques RBF, MLP, and ANFIS with MLR and MNLR for predicting grade-control scour hole geometry, *Engineering Applications of Computational Fluid Mechanics*, 13:1, 529-550, DOI: [10.1080/19942060.2019.1618396](https://doi.org/10.1080/19942060.2019.1618396)

To link to this article: <https://doi.org/10.1080/19942060.2019.1618396>



© 2019 The Author(s). Published by Informa UK Limited, trading as Taylor & Francis Group



Published online: 22 Jun 2019.



Submit your article to this journal [↗](#)



Article views: 88



View Crossmark data [↗](#)

Comparative analysis of soft computing techniques RBF, MLP, and ANFIS with MLR and MNLr for predicting grade-control scour hole geometry

Hossien Riahi-Madvar^a, Majid Dehghani^b, Akram Seifi^a, Ely Salwana^c, Shahaboddin Shamshirband^{d,e}, Amir Mosavi^{f,g} and Kwok-wing Chau^h

^aDepartment of Water Science & Engineering, Faculty of Agriculture, Vali-e-Asr University of Rafsanjan, Rafsanjan, Iran; ^bTechnical and Engineering Department, Faculty of Civil Engineering, Vali-e-Asr University of Rafsanjan, Rafsanjan, Iran; ^cInstitute of Visual Informatics, Universiti Kebangsaan Malaysia, Malaysia; ^dDepartment for Management of Science and Technology Development, Ton Duc Thang University, Ho Chi Minh City, Vietnam; ^eFaculty of Information Technology, Ton Duc Thang University, Ho Chi Minh City, Vietnam; ^fInstitute of Automation, Kando Kalman Faculty of Electrical Engineering, Obuda University, Budapest-, Hungary; ^gSchool of the Built Environment, Oxford Brookes University, Oxford, UK; ^hDepartment of Civil and Environmental Engineering, Hong Kong Polytechnic University, Hong Kong, People's Republic of China

ABSTRACT

The main aims and contributions of the present paper are to use new soft computing methods for the simulation of scour geometry (depth/height and locations) in a comparative framework. Five models were used for the prediction of the dimension and location of the scour pit. The five developed models in this study are multilayer perceptron (MLP) neural network, radial basis functions (RBF) neural network, adaptive neuro fuzzy inference systems (ANFIS), multiple linear regression (MLR), and multiple non-linear regression (MNLr) in comparison with empirical equations. Four non-dimensional geometry parameters of scour hole shape are predicted by these models including the maximum scour depth (S), the distance of S from the weir (XS), the maximum height of downstream deposited sediments (hd), and distance of hd from the weir (XD). The best results over train data derived for XS/Z and hd/Z by the MLP model with R^2 are 0.95 and 0.96 respectively; the best predictions for S/Z and XD/Z are from the ANFIS model with R^2 0.91 and 0.96 respectively. The results indicate that the application of MLP and ANFIS results in the accurate prediction of scour geometry for the designing of stable grade control structures in alluvial irrigation channels.

ARTICLE HISTORY

Received 1 February 2019
Accepted 9 May 2019



KEYWORDS

scour geometry; alluvial channels; artificial intelligence; grade control structure; big data; radial basis functions

1. Introduction

Grade control structures are commonly used in irrigation channels for regulating water level, supplying required head upstream of weirs, measuring flow rate, enhancing water quality by reducing erosion, and preventing degradation in a bed channel of alluvial materials (Najafzadeh, 2015). The performance of the irrigation channel will increase by using these structures. Water flowing from the top crest of the weir (as one of the grade control structures) creates a vortex and increases flow velocity downstream of hydraulic structures that result in local scour (Mohammadpour, 2017; Sarkar & Dey, 2004). Local scour creates holes downstream of a weir and its dimensions increase gradually and become unbalanced, which causes the failure of the hydraulic structures or weir (Goel & Pal, 2009). Therefore, it is necessary that adequate effort and attention are given to the safe design of the foundations of hydraulic structures (Sarkar & Dey,

2004; Termini & Sammartano, 2012). There are various hydraulic and geotechnical factors that have an effect on the local scour downstream of water level adjusting structures in erodible beds. Figure 1 shows a plan view of local scour on an alluvial bed downstream of a water level control structure at the equilibrium stage (D'Agostino & Ferro, 2004). Local sediment transport is actively done throughout the developing stage of the local scour pit. With approaching the equilibrium state, this phenomenon becomes a 'purely hydraulic' mechanism, where mass balance among removed and deposited particles at the downstream creates the scour hole profile (D'Agostino & Ferro, 2004). Generally, the scour around the level control structures is essentially complex progress because of the three-dimensional flow patterns relating to alluvial bed materials and erodible beds. In conjunction with Figure 1, it is clear that the four geometric parameters that define the local scour hole dimensions

CONTACT Shahaboddin Shamshirband  Shahaboddin.shamshirband@tdtu.edu.vn  Department for Management of Science and Technology Development, Ton Duc Thang University, Ho Chi Minh City, Vietnam

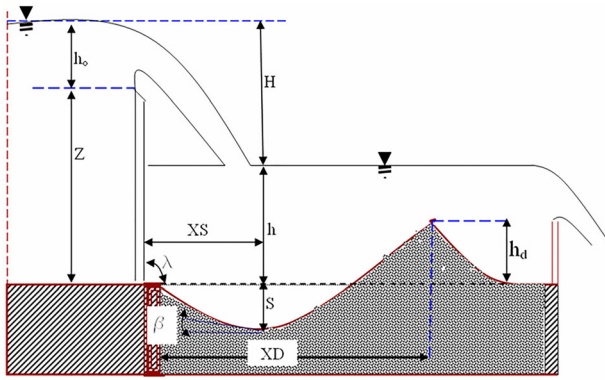


Figure 1. Schematic view of scour geometry downstream of grade control structures.

and geometry are: maximum scour depth (S); distance of S from the weir (XS); maximum height of downstream deposited sediments (h_d); and distance of h_d from the weir (XD). An accurate estimation of these four scour hole dimensions around the water level adjusting structures is one of the most important stages in grade control structure design and is the main contribution of the present study.

The scour mechanism for grade control structures is complex and is usually studied by regression analysis or simple empirical equations. Various investigators have widely studied the local scour process around the water level control structures based on experimental and prototype observations (Guan, Melville, & Friedrich, 2016; Lenzi, Marion, Comiti, & Gaudio, 2002; Lu, Hong, Chang, & Lu, 2013; Marion, Tregnaghi, & Tait, 2006; Pagliara & Kurdistani, 2013; Scurlock, Thornton, & Abt, 2011). Mason and Arumugam (1985) and Hoffmans and Verheij (1997) proposed many regression equations for estimating the final scour depth. Gaudio, Marion, and Bovolin (2000) presented an equation to predict the depth and length of a scour pit by using sediment particle size and morphological length. Lenzi, Marion, and Comiti (2003) investigated many water level adjustment structures in mountain rivers to assess the effects of a water flow jet on the progress of scouring. Pagliara (2007) developed a regression equation to characterize the scour pit shape. Kumar and Sreeja (2012) investigated the scour depth prediction by several experimental equations presented in the literature by using experimental and field data. In regard to these results, it is concluded that the predictive equations for scour depth cannot be used generally for all ranges of total water head and flow discharge. Melville and Lim (2014) collected some laboratory data and developed a formula to estimate the scour dimension for a horizontal 2D jet. Rajaei, Esmaili Varaki, and Shafei Sabet (2019) studied the influences of various factors on

local scour downward of water level adjusting structures in trapezoidal and rectangular labyrinth plan form.

Prediction of local scour hole geometry is a major and critical subject in water resource engineering for preventing excessive channel bed degradation and protecting the stability of water level adjustment structures (Lauccelli & Giustolisi, 2011) in alluvial channels. The scour process around the level adjustment structures can damage these structures and downstream channel geometry (Najafzadeh, 2015). Traditional and statistical methods such as regression methods are limited to the studies in the experimental and field conditions. Sometimes, this concern does not lead to providing the accurate prediction for scour depth. Consequently, the equations that are extended based on these methods cannot be applicable in most cases (Hooshyaripor, Tahershamsi, & Golian, 2014). Hence, developing new techniques for modifying traditional physical-based analysis is crucial. Recently, using artificial soft computing models such as artificial neural network (ANN) simulation models and a fuzzy based model, adaptive neuro fuzzy inference system (ANFIS) has been introduced as an accurate learning scheme for modeling complex phenomena in different aspects of hydraulic and water engineering problems (Bateni & Jeng, 2007; Chau, 2017; Hameed et al., 2017; Moazenzadeh, Mohammadi, Shamshirband, & Chau, 2018; Taormina, Chau, & Sivakumar, 2015; Wan Mohtar, Afan, El-Shafie, Bong, & Ab. Ghani, 2018; Wu & Chau, 2011; Yaseen, El-Shafie, Afan, Hameed, Wan Mohtar & Hussain, 2016; Yaseen, Sulaiman, Deo, & Chau, 2019; Zounemat-Kermani, Beheshti, Ataie-Ashtiani, & Sabbagh-Yazdi, 2009). These artificial intelligence methods benefit from the simplicity, ability, and proper results of modern and advanced computers (Nguyen, Ahn, & Park, 2018; Salmasi, Yildirim, Masoodi, & Parsamehr, 2013), knowledge based and data based nature, predictions without need of model form, and greater endurance over the data errors (Azamathulla, 2005; Bateni & Jeng, 2007) than statistical models. For instance, Liriano and Day (2001) reported higher performance of the ANN method in estimating scour dimension near a culvert in comparison to the existing empirical equations. Goel and Pal (2009) compared the results of support vector machines (SVM) and ANN models with an empirical equation for modeling scour. Based on the results, the SVM model showed better performance than both ANN and empirical equations for scour prediction. Azamathulla (2012) studied a gene-expression programming (GEP) model for estimating scour depth at the downstream of sills and the results compared to estimations of existing equations in Chinnarasri and Kositgittiwong (2008). The GEP model had better results. Najafzadeh (2015) used a hybrid model of an ANFIS based-group

model of data handling (NF-GMDH) combined with the particle swarm optimization (PSO) to simulate the scour depth after the weirs. Results showed the hybrid NF-GMDH-PSO model produces higher accuracy for estimating scour depth than the evolutionary polynomial regression (EPR) and GEP models. Elnikhely (2018) investigated the accuracy of ANFIS and SVM models to simulate scour depth after the rectangular channels. Based on the results, the ANFIS model showed more accuracy than the SVM model. Karbasi and Azamathulla (2017) applied several models including ANN, SVM, ANFIS, GEP, and GMDH of ANN and ANFIS to estimate scour hole depth after a channel gate. Comparison of results proved that the ANN model has higher performance than the other models with $RMSE = 0.869$.

As mentioned above, different artificial intelligence models were used to simulate scour around the water level control structures. But other geometric parameters such as X_S , h_d , and XD are not considered in the scour hole modeling of these structures. Hence, the objectives of this study are: (1) collecting previous observations on local scour hole patterns in alluvial beds at the downstream of grade control structures from published literature; (2) using different models of multilayer perceptron neural networks (MLP), radial basis functions (RBF) of ANN, ANFIS, multi-linear, and non-linear regression (MLR, MNLR) to predict geometric parameters of local scour at the downstream of grade control structures; and (3) predicting four geometric parameters of depth, width, and length of scour hole and deposited height of sediment at the downstream of grade control structures due to their importance in the grade control design and stability of the hydraulic structure. In other words, in this study the authors use five models to predict a three-dimensional pattern of scour hole geometry and dimensions around the water level and control structures based on comparative evaluations.

2. Material and methods

The main contribution of the present study is to collect previously published data on patterns of local scour at alluvial beds downstream of water level control structures, and develop new techniques of artificial intelligence with regard to providing better predictions. Not only the depth of scour, but also the scour pit width and length, as well as the deposited height of sediment at downstream, were used for simulation in the present paper in regard to their importance in the grade control design and stability of the structure. In other words, in this study the authors used five models to predict a three-dimensional pattern of scour hole dimensions. In this section, the theoretical dimensional analysis of

scour concepts, study literature, and some previously published regression equations of scour hole dimensions are described. After that, MLP, RBF, ANFIS, MLR, and NMLR models are considered. Also, the data set and hydraulic parameters that are used in the model developments of the study and available ranges of the effective variables are presented.

2.1. Theoretical and dimensional analysis

There are several hydraulic, morphologic, and geotechnical features leading to the scour pit formation around the water level control structures. Referring to Figure (1) these affective and independent parameters include discharge per width q (Q/B), fall height z , weir width b , tail water depth h , distance from the downstream edge of the weir and the scour pit crest XD , acceleration due to gravity g , upstream side angle of scour b , face angle of downstream edge l , water depth above the weir y_0 , differences in height (m) from upstream, and downstream water level H . Moreover, d_{50} is diameter than which 50% of deposited sediment particles are finer; and d_{90} is diameter than which 90% of deposited sediments are finer. Four major dependent scour variables are: maximum scour depth S and its longitudinal location X_S ; and maximum height of downstream mound h_d and its distance from the weir XD .

Based on the above factors and Figure (1), the scour process, because of the erosive force of flow, can be explained mathematically by the next equation:

$$F(x, z, b, B, Q, h, h_o, g, \rho, \rho_s, d_m, d_{90}, \beta, \lambda) = 0 \quad (1)$$

Where F is the functional symbol and x scour variable. S , X_S , h_d , XD , and the other parameters are defined previously. By using a dimensional analysis technique Equation (1) can be written in dimensionless form:

$$\frac{x}{z} = \phi \left(\frac{b}{z}, \frac{h}{H}, \frac{B}{b}, Q/bz, \sqrt{gd_m \left(\frac{\rho_s - \rho}{\rho} \right)}, \beta, \lambda, \frac{d_{90}}{d_m} \right) \quad (2)$$

Referring to Equation (2), the input vector of all models which are used in this study is:

$$\frac{b}{z}, \frac{h}{H}, \frac{B}{b}, Q/bz, \sqrt{gd_m \left(\frac{\rho_s - \rho}{\rho} \right)}, \theta, \frac{d_{90}}{d_m}$$

and the only output variable is one of the scour variables: (S/z) , (X_S/z) , (h_d/z) , (XD/z) . In this paper for any of these scour variables a separate model was developed and these variables are estimated separately.

The over-fall jet splits into two roller jets that rotate inversely. The upstream wave slaves through the falling and the combining jet. The downstream jet moves

upward and creates a region of sediment deposition as water flows downward (Sui, Faruque, & Balachandar, 2008).

Based on the detailed literature review and data analysis it is concluded that the idea of a final equilibrium scour hole for all of the practical cases is valid and several investigators used the similar dimensional analysis in conjunction with regression technique and hydraulic models to develop empirical equations for the estimation of local scour downstream of weirs (Mason & Arumugam, 1985). In Table 1 some of the most important of these equations have been presented. Recently, several studies used artificial intelligence for modeling complicated hydraulic phenomenon in water resource management and civil-environmental engineering (Chang, Azamathulla, Zakaria, & Ab Ghani, 2012; Dehghani, Saghafian, Nasiri Saleh, Farokhnia, & Noori, 2014; Dehghani et al., 2019; Juahir, Zain, Aris, Yusoff, & Mokhtar, 2010; Khan, Azamathulla, & Tufail, 2012; Najah, El-Shafie, Karim, & El-Shafie, 2013; Najafzadeh, Saberi-Movahed, & Sarkarmaryan, 2018; Pandey, Zakwan, Sharma, & Ahmad, 2019; Seifi & Riahi-Madvar, 2019). In this study the MATLAB 2014 environment is used for developing soft computing models and SPSS 8 is used for linear and non-linear model developments.

2.2. Artificial neural networks

2.2.1. Multi-layer perceptron

Neural networks (NNs) are stimulated by biological neurons to accomplish brain-like calculations by enormously

direct connective artificial neurons (Riahi-Madvar & Seifi, 2018). A remarkable development in the importance of this computational framework has happened since an accurately laborious theoretical background for NNs, i.e. error back propagation was introduced (ASCE, 2000). Multi-layer perceptron (MLP) neural networks are the usual and common kind of ANNs and have been effectively used for adaptive simulation of non-linear problems in real world mechanisms. In these models, the linearly weighted input vector of a node is delivered to the hidden layer and transformed by the activation function of the hidden layer. The activation function provides the model non-linearity estimation capability. MLP is possibly the greatest common type of all the ANNs and is broadly used in relation estimation, future prediction, and simulation of pattern grouping. The neurons are organized in a layered structure with three major layers, which contains input (containing input function), hidden, and final output layers. The layers are composed of a number of neurons which are the essential structure of the model. The input vector which includes independent parameters of the phenomenon is entered to the input layer. The hidden layer characterizes the nonlinear relations of the inputs. The final adjusted model includes hidden layers subject to the phenomenon's degree of complexity. In the last layer of the model, the output layer is made up of the dependent parameters of the phenomenon. The learning procedure drives from the first layer to the hidden layer, and progresses to the latest layer. The unidirectional connection between the nodes uses results of nodes in a previous layer as the input

Table 1. Available empirical equations for the hole scour dimensions prediction.

Ref.	Eq. No.	Equation	Author (year)
[8]	(3)	$\frac{XD}{z} = 3.55 \sqrt[3]{\frac{q^2}{g}} + 0.34$	D'Agostino (1994)
[36]	(11)	$\frac{s}{z} = \frac{S}{\left(\frac{q^2}{g}\right)^{1/3}} = (6.42 - 3.1H^{0.1})g^{-H/600}$	Yen (1987)
[8]	(12)	$\frac{s}{z} = 0.540 \left(\frac{b}{z}\right)^{0.593} \left(\frac{h}{H}\right)^{-0.126} \left(\frac{d_{90}}{d_{50}}\right)^{-0.856}$ $\times \left(\frac{b}{B}\right)^{-0.751} \left(Q/bz \sqrt{gd_{50} \left(\frac{\rho_s - \rho}{\rho}\right)}\right)^{0.544}$	D'Agostino and Ferro (2004)
[8]	(13)	$\frac{s}{z} = 0.975 \left(\frac{h_0}{z}\right)^{0.863}$	D'Agostino and Ferro (2004)
[8]	(14)	$\frac{XS}{z} = 1.616 \left(\frac{b}{z}\right)^{0.662} \left(\frac{h}{H}\right)^{-0.117} \left(\frac{b}{B}\right)^{-0.478}$ $\times \left(Q/bz \sqrt{gd_{90} \left(\frac{\rho_s - \rho}{\rho}\right)}\right)^{0.455}$	D'Agostino and Ferro (2004)
[8]	(15)	$\frac{XD}{z} = 5.828 \left(\frac{b}{z}\right)^{0.241} \left(\frac{h}{H}\right)^{0.041} \left(\frac{b}{B}\right)^{0.057}$ $\times \left(Q/bz \sqrt{gd_{50} \left(\frac{\rho_s - \rho}{\rho}\right)}\right)^{0.508} \left(\frac{d_{90}}{d_{50}}\right)^{-1.077}$	D'Agostino and Ferro (2004)
[8]	(16)	$\frac{h_d}{z} = 2.780 \left(\frac{h}{H}\right)^{0.061} \left(\frac{b}{B}\right)^{0.794}$ $\times \left(Q/bz \sqrt{gd_{90} \left(\frac{\rho_s - \rho}{\rho}\right)}\right)^{0.764} \left(\frac{d_{90}}{d_{50}}\right)^{-2.489}$	D'Agostino and Ferro (2004)

of the nodes in the next one. The MLP model uses the supervised training algorithm which associates the simulated results to the observed values and then readapts the weights in the mode by backward propagation of error (Ham & Kostanic, 2001; Riahi-Madvar & Seifi, 2018).

2.2.2. Error back-propagation procedure

In the training stage of the MLP model, the data provided to an ANN model is spread layer-by-layer starting at the first layer (input) to the hidden layers and finally to the last one (output). The procedure, in a repetitious approach designed to apply repetitive improvements to the weights, includes the steps of giving an input to the model, creation estimates to the result z_{pk} , and after that evaluating the calculated result to the observed targets t_{pk} . The overall error (Equation 3), by considering the squared error of estimated and observed values of the pattern p , is calculated as:

$$E_p = \sum_{k=1}^N (t_{pk} - z_{pk})^2 = \sum_{k=1}^N v_{pk}^2 \quad (3)$$

in which v_{pk} is the error of the result k of observation p . The aim of learning procedure is to provide an adequate number of matchless input–output jointed couples P , that are joined with an appropriate procedure for weight modification, and creates a collection of adjusted weights by minimizing the overall model error. As identified mostly by previous researches, the neural networks offer an arbitrary planning among the input set to the output set by imitating the natural perception development of human intelligence (Azamathulla, 2005). The Levenberg-Marquardt (LM) is used for MLP training in this study as the most accurate model (Choubin, Malekian, Samadi, Khalighi-Sigaroodi, & Sajedi-Hosseini, 2017).

2.2.3. Radial basis functions

ANNs with radial basis functions (RBF) are one of the usual function approximations. One of the most important traits of RBF models is the one type having a high-dimensional-space model with a nonlinear structure that can be simply fragmented by using a collection of a group of RBF models; moreover the RBF models are the RBF models have the capability of rapidly learning (Zounemat-Kermani et al., 2009). In an RBF model the input layer is composed of input parameters. In spite of the MLP model, in the RBF model there is only one hidden layer, which is composed of an arbitrary number of units. Any unit in a hidden layer has its radial basis function as an activation function (Khadangi, Madvar, & Ebadzadeh, 2009). The output of the hidden layer $Z_j(x)$ estimates the distance between input to the center of the radial basis function and images this distance on to the

activation function as follows (Khadangi et al., 2009):

$$z_j(x) = \exp\left(-\frac{\|x - \mu_j\|^2}{2\sigma_j^2}\right) \quad (4)$$

in which x is the input parameter, μ_j is the center of RBF in j^{th} neuron of hidden layer, $\|x - \mu_j\|$ is the Euclidean distance from the center of the RBF to the input, and σ_j is a factor for adjusting the softness features of the RBFs. The model result is calculated as the sum of linear weights $z_j(x)$:

$$y_l = \sum_{j=0}^J w_{lj} z_j(x) \quad z_0(x) = 1 \quad (5)$$

in which y_l is the l^{th} element of the result layer, w_{lj} is the weight of the j^{th} node of hidden layer to the l^{th} node of result layer. $Z(x) = 1$ in Equation (5) shows the Constant w_{l0} in the model.

2.3. Adaptive neuro fuzzy inference systems

The ANFIS model is known as the acronym of the adaptive neuro fuzzy inference system. ANFIS is an adaptive fuzzy based model that is developed by using the computation ability of the ANNs (Jang & Gulley, 1995). The ANFIS is a Sugeno type of fuzzy model that has a promoting system configuration using two different clustering methods: grid partition and subtractive clustering (Sanikhani, Kisi, Kiafar, & Ghavidel, 2015). Figure 2 displays a Sugeno fuzzy system that has two input parameters, one output parameter as the result, and two rules. The corresponding ANFIS structure of this system is also presented in Figure 2 (Rafiei-Sardooi et al., 2018; Seifi & Riahi, 2018). Its rules are:

- Rule 1: If x is A_1 and y is B_1 Then $f = p_1x + q_1y + r_1$
 Rule 2: If x is A_2 and y is B_2 Then $f = p_2x + q_2y + r_2$

The output of node i in j layer of ANFIS model is O_{ij} (Jang & Gulley, 1995). Moreover, its layers from input to output are:

First layer, input variables: in this layer any input is imagined to fuzzy set by corresponding to the membership degree of bell shape membership function (Zadeh, 1965):

$$O_i^1 = \frac{1}{1 + [(x - c_i)/a_i]^{2b_i}} \quad (6)$$

X is the input variable i , and c_i , b_i and a_i are the constants of fuzzy membership function and usually called if (condition) parameters.

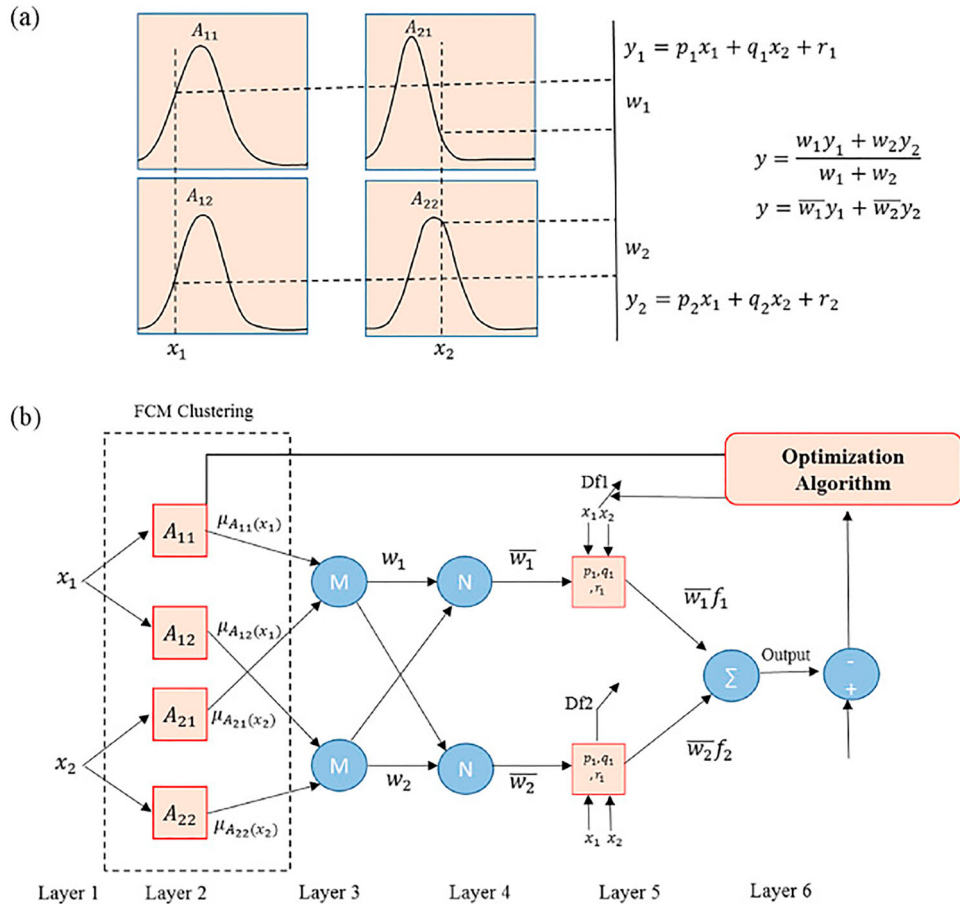


Figure 2. The structure of the Sugeno fuzzy system, its membership function, and equivalent ANFIS structure.

Second layer, rule grids: the grade of activation of incorporated rules is evaluated:

$$O_i^2 = w_i = \mu_{A_i}(x) \times \mu_{B_i}(y), i = 1, 2$$

in which the $\mu_{A_i}(x)$ is the membership degree of input variable x in A_i , and $\mu_{B_i}(x)$ is for y in B_i respectively.

Third layer, intermediate grids: this layer calculates relative activation degree:

$$O_i^3 = w_i^n = \frac{w_i}{w_1 + w_2}, \quad i = 1, 2 \quad (7)$$

and the w_i^n is the normalization of each rule i membership degree.

Fourth layer, consequent grids: here the output of layers is determined:

$$O_i^4 = w_i^n f_i = w_i^n \cdot (p_i + q_i + r_i), \quad i = 1, 2$$

The r_i , q_i , and p_i are the regulatory constants that should be calculated in the optimization procedure and known as the result constants.

Fifth layer, final result layer: the overall result of the system is evaluated

$$O_i^5 = \sum w_i^n f_i = \frac{\sum w_i f_i}{\sum w_i} \quad (8)$$

in this study by comparing different structures. Finally, the gbellmf: generalized bell-shaped membership function is used with a three membership function for each rule and the hybrid learning algorithm is used for training the ANFIS model.

2.4. Multi-linear regression

Another model that is used in the present paper is linear regression. In the case that the output parameter Y is related to the m input parameters X_1, X_2, \dots, X_m and a linear relation is supposed to show the dependences of Y to X_i , the multiple linear equation of Y is $Y = a + b_1 \times x_1 + b_2 \times x_2 + \dots + b_m x_m$.

y in this model displays the estimated value of the parameter Y in regard to the input parameters of $X_1 = x_1, X_2 = x_2, \dots, X_m = x_m$. The multi-linear regression constants a, b_1, b_2, \dots, b_m are determined by

minimizing the sum of the e_{yi} differences of measured values from the model determined by the regression model (Kisi & Cobaner, 2009):

$$\sum_{i=1}^N e_{yi}^2 = \sum_{i=1}^N (y_i - a - b_1x_{1i} - b_2x_{2i} - b_mx_{mi})^2 \quad (15)$$

In the present study, the constants a, b_1, b_2, \dots, b_m are derived by least squares procedure (Kisi & Cobaner, 2009). The multi-linear regression model of scour on an alluvial bed downstream of water level control structures is:

$$\frac{x}{z} = a_0 + a_1 \frac{b}{z} + a_2 \frac{h}{H} + a_3 \frac{b}{B} + a_4 \left(\frac{Q}{bz} \sqrt{gd_m \left(\frac{\rho_s - \rho}{\rho} \right)} \right) + a_5 \frac{d_{90}}{d_m} \quad (9)$$

2.5. Multi-non-linear regression

Because of the complexity of the scour process the non-linear regression models are used. The multivariable non-linear least square regression (MNLRL) model is used for the estimation of scour dimensions. If the output parameter f is to be a function of input parameters x_i ($i = 1, \dots, n$):

$$f = f(x_1, x_2, \dots, x_n) \quad (10)$$

by using the polynomials, the functional form of this equation is (Ramamurthy, Qu, & Vo, 2006):

$$f = g_1(x_1) \cdot g_2(x_2) \dots g_n(x_n) = \prod_{i=1}^n g_i(x_i) \quad (11)$$

in which $g_i(x_i) =$ several degree polynomial equation.

If f_k is to be the observed value related to x_{ik} , the sum of the square errors minimization by least square method is used to derive nonlinear regression coefficients a_{ij} :

$$\delta^2 = \sum_{k=1}^s (f - f_k)^2 \quad (12)$$

In this study after several preliminary trials the following Multi-Non-Linear Regression equation was selected for

scour modeling:

$$\frac{x}{z} = a \left(\frac{b}{z} \right)^b \left(\frac{h}{H} \right)^c \left(\frac{b}{B} \right)^d \left(\frac{Q}{bz \sqrt{gd_m \left(\frac{\rho_s - \rho}{\rho} \right)}} \right)^e \left(\frac{d_{90}}{d_m} \right)^f \quad (13)$$

2.6. The data set and empirical equations

Estimation of scour hole dimensions on an alluvial bed with hydraulic water level structures using the equations of Table 1, MLR, MNLRL, MLP, RBF, and ANFIS models needs hydraulic and geometry experimental data. A data bank of published literature was prepared and models developed. The data is gathered such that it includes all necessary variables in previous studies. Table 2 presents the features of implemented data and variables. In all of the collected data the b and l were constant (90°) and eliminated from the effective variables. A reliable data set involving 226 documented tests of scour geometry downstream of water adjusting and grade control structure is compiled from literature. The data set are used from published literature such as (D’Agostino & Ferro, 2004). Seventy-five percent of the database is used for the training stage of models; the remaining 25% is used for the testing of models, which in all of the models, training (calibration), and testing (prediction) data sets were similar (except for RBF). Training and testing subsets are divided randomly and the final best structure of ANN and ANFIS models were found through a trial and error process. Subsequently, different models with different layers and parameters were developed and finally the optimum structure of ANN and ANFIS models was determined and the results of optimum model compared with other models. All the data was dimensionless and based on dimensionless parameters of Equation (2). Furthermore, in ANN models based on the maximum and minimum values, the dimensionless variables normalized between (0.2 - 0.8). The dataset of the present study is presented in Appendix 1.

The empirical equations are the equations that have been developed by different authors in previous literature. Those used in the present study are presented in Table 1. In Table 1 the available empirical equations for the hole scouring dimensions predictions with their

Table 2. The statistical indices of the collected data set.

Author (year)	Number of data	Range of hd (m)	Range of XD (m)	Range of XS (m)	Range of S (m)
Veronese (1937)	36	*****	*****	*****	.05-.22
Mossa (1998)	19	*****	*****	0.17-.67	.035-.145
D’Agostino (1994)	114	0.045-0.255	0.43-1.75	.215-.705	.045-.85
D’Agostino and Ferro (2004)	113	*****	*****	*****	.15-.65
Falciai and Giacomini (1978)	29	*****	*****	*****	.4-3.5
Lenzi, Marion, Comiti, and Gaudio (2000)	13	*****	*****	*****	.016-.053
Scimemi (1939)	3	*****	*****	*****	5-40

Table 3. Empirical equation results in the estimation of scour hole dimensions.

Statistical parameter						Scour parameter	Author (year)
NSE	TS100%	AARE (%)	MAE	RMSE	R ²		
-14.95	1686.6	276.5	0.945	2.01	0.8	S	Yen (1987)
-14.56	982.45	91.63	0.57	1.793	0.5145	S/Z	D'Agostino and Ferro (2004)
0.47	434.6	33.20	0.144	0.326	0.688	S/Z	D'Agostino and Ferro (2004)
0.69	56.63	17.93	0.329	0.724	0.734	XS/Z	D'Agostino and Ferro (2004)
0.75	171.5	32.8	0.054	0.067	0.79	h _d /Z	D'Agostino and Ferro (2004)
-0.52	63.37	47.87	0.95	1.087	0.865	XD/Z	D'Agostino (1994)
-12.59	44.99	12.82	0.192	0.239	0.9113	XD/Z	D'Agostino and Ferro (2004)

corresponding references are provided. As these empirical equations are not developed in the present study and because of the limit of the size of the paper, they are not described more here. However, readers can find more details on the mentioned references. Instead, in this study, new equations are developed by using MLR and MNLR which are fully described in the previous sections.

2.7. Statistical parameters

The results of the implemented six methods are evaluated by several statistical indices such as: correlation coefficient (R²); root mean square error (RMSE); and mean absolute error (MAE). These indices illustrate the average performance of model prediction errors. They are overall information and do not provide details about the distribution of prediction error results. In order to assess the error distribution of modes, two further statistical indices that can accurately evaluate the distribution percent of model results are established: average absolute relative error (AARE) and threshold statistics index (TS). These not only illustrate the performance of a model in the estimation of scour dimensions by a single value, but also display the distribution of errors over all of the predictions. The TS_x value for x% of estimations illustrates the error distribution of estimated values of different models and is calculated for different AARE values. The value of TS for x% of estimation is calculated by

$$TS_x = \frac{Y_x}{n} \cdot 100 \tag{14}$$

in which Y_x is the number of estimations (from total number of n) for each AARE value which is less than x%. Mathematical equations of RMSE, R², NSE, MAE, and AARE statistical parameters are (Sanikhani et al., 2018):

$$RMSE = \left[\frac{\sum_{i=1}^n (O_i - P_i)^2}{n} \right]^{0.5} \tag{15}$$

$$R^2 = \left[\frac{\sum_{i=1}^n (O_i - \bar{O})(P_i - \bar{P})}{\sqrt{\sum_{i=1}^n (O_i - \bar{O})^2} \sqrt{\sum_{i=1}^n (P_i - \bar{P})^2}} \right]^2$$

$$NSE = 1 - \frac{\sum_{i=1}^n (O_i - P_i)^2}{\sum_{i=1}^n (O_i - \bar{O})^2} \tag{16}$$

$$MAE = \frac{1}{n} \sum_{i=1}^n |P - O_i| \tag{17}$$

$$AARE\% = \frac{1}{n} \sum_{i=1}^n \frac{O_i - P_i}{O_i} * 100 \tag{18}$$

3. Results and discussions

This section provides the evaluation of the developed methods in the prediction of scour hole geometry dimensions and the statistical parameters for accuracy assessment are provided. The final results of six methods of empirical relations, MLP, RBF, ANFIS, MLR, and MNLR are presented, analyzed, compared and discussed.

Table 4. Results of the MLR model in the prediction of scour hole dimensions.

Statistical parameter						Scour parameter	Stage
NSE	TS100%	AARE (%)	MAE	RMSE	R ²		
0.66	530.82	75.19	0.185	0.289	0.659	S/Z	Calibration
0.76	4.434	13.932	0.261	0.635	0.761	XS/Z	Calibration
0.96	42.95	7.98	0.13	0.174	0.961	XD/Z	Calibration
0.94	81.54	12.74	0.0242	0.0334	0.944	hd/Z	Calibration
0.43	287.01	65.84	0.141	0.192	0.462	S/Z	Testing
0.61	119.71	18.54	0.38	0.803	0.68	XS/Z	Testing
0.87	64.25	9.74	0.142	0.182	0.88	XD/Z	Testing
0.87	136.91	22.166	0.0288	0.0452	0.873	hd/Z	Testing

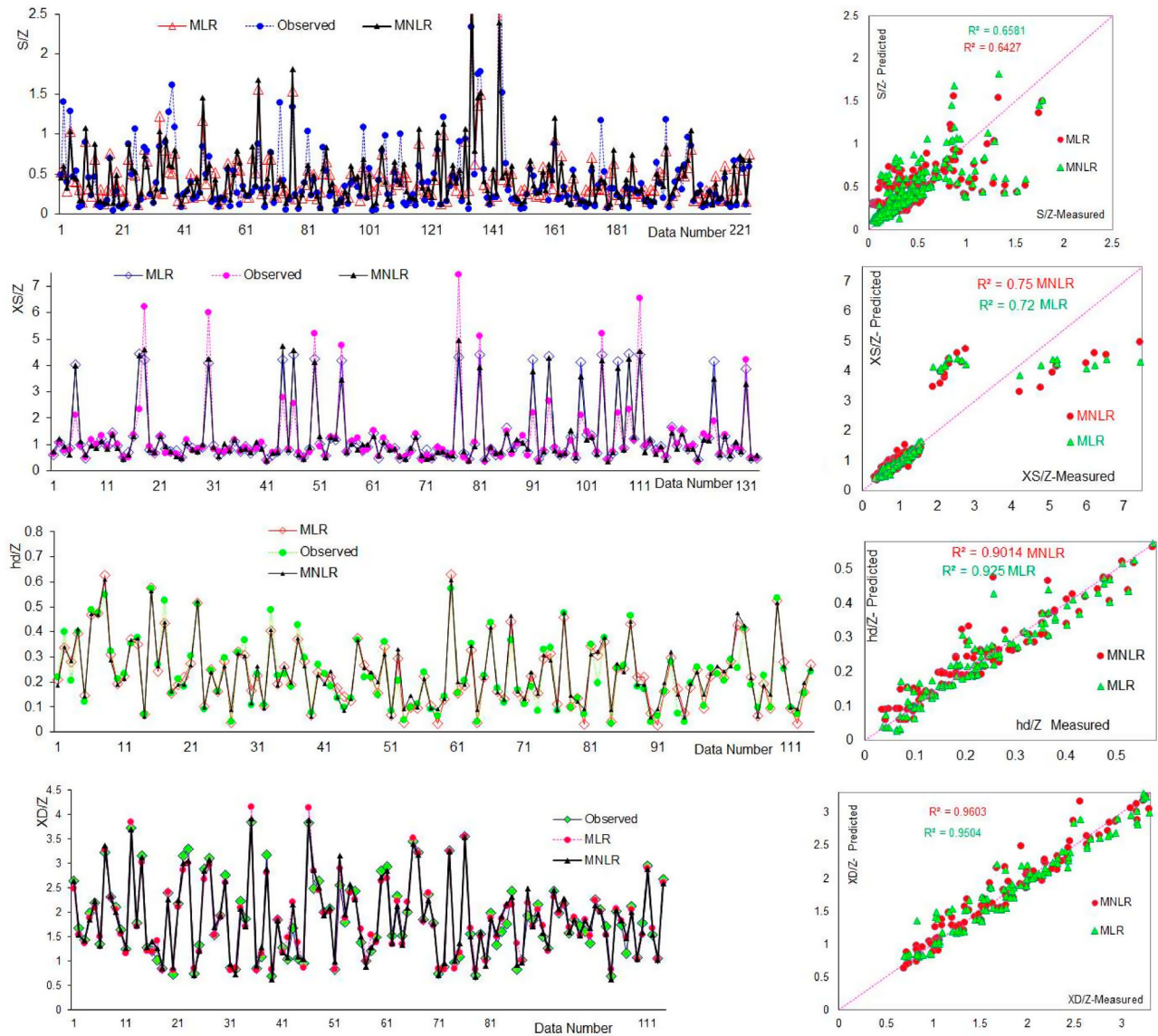


Figure 3. Comparison of estimated and observed values of score hole geometry by MLR and MNLN.

3.1. Results of empirical equations

One of the usual approaches for the estimation of grade control scour is the application of the published empirical equations. There are several empirical equations presented to calculate the depth and height of scour depth/deposits. In this paper, to assess the accuracy of the MLR, RBF, and ANFIS with observed values, comparisons are also done with some of the best-known previously published equations (Table 1).

The results of empirical equations in Table 1 for the estimation of score hole geometry are determined using the entire data set. Table 3 presents the statistical indices of the empirical equations of Table 1. As is clear from results in Table 3, none of these empirical equations provides acceptable estimations for scour geometry and

have substantial errors in contrast with the observations. The superlative empirical equation for XD/Z is the D'Agostino and Ferro (2004) equation with $R^2 = 0.9113$, RMSE = 0.239, MAE = 0.192, AARE = 44.9%, and $TS_{100\%} = 44.99$. This shows that for 44.99% of estimated values, the prediction error of model outputs are greater than 100%. That is very high and indicates the poor performance of available empirical equations. It is seen that while the location of the maximum deposits (XD/Z) is estimated with an acceptable accuracy, the S/Z, hd/Z, and XS/Z are estimated with less accuracy. The performance of empirical equations for other parameters of a scour hole is very poor and could not be used as accurate design methods; new methods are required. The values of these statistical indices in four scour parameters show the weak prediction of previous empirical equations for

Table 5. Results of the MNL model in the prediction of scour hole dimensions.

Statistical parameter						Scour parameter	Stage
NSE	TS100%	AARE (%)	MAE	RMSE	R ²		
0.66	435.949	45.02	0.161	0.288	0.665	S/Z	Calibration
0.77	88.74	18.392	0.303	0.622	0.771	XS/Z	Calibration
0.87	28.7	6.46	0.105	0.146	0.972	XD/Z	Calibration
0.93	111.34	17.52	0.029	0.038	0.93	hd/Z	Calibration
0.53	259.82	38.01	0.1085	0.175	0.576	S/Z	Testing
0.69	84.05	20.993	0.394	0.713	0.7135	XS/Z	Testing
0.97	28.163	8.116	0.131	0.181	0.88	XD/Z	Testing
0.81	150.73	26.52	0.035	0.053	0.84	hd/Z	Testing

scour depth around the grade control structures. It is noticeable that the empirical equations of D’Agostino and Ferro (2004) were established by using the dataset which is used in present study, and that authors do not recalibrate these equations.

3.2. Results of the MLR model

Based on the non-dimensional parameters of Equation (2), four multi-linear regression equations are developed and their coefficients derived, which are:

$$\frac{S}{z} = -0.482 + 0.021 \frac{b}{z} + 0.14 \frac{h}{h_0 + z - h} + 0.631 \frac{B}{b} + 0.071 \left(Q/bz \sqrt{gd_m \left(\frac{\rho_s - \rho}{\rho} \right)} \right) + 0.112 \frac{d_{90}}{d_m} \quad (19)$$

$$\frac{XS}{z} = -0.942 + 0.661 \frac{b}{z} + 0.037 \frac{h}{h_0 + z - h} + 2.728 \frac{B}{b} + 0.836 \left(Q/bz \sqrt{gd_m \left(\frac{\rho_s - \rho}{\rho} \right)} \right) - 0.361 \frac{d_{90}}{d_m} \quad (20)$$

$$\frac{h_d}{z} = 0.073 + 0.447 \frac{b}{z} - 0.013 \frac{h}{h_0 + z - h} + 0.444 \left(Q/bz \sqrt{gd_m \left(\frac{\rho_s - \rho}{\rho} \right)} \right) + 0.021 \frac{d_{90}}{d_m} - 0.531 \frac{B}{b} \quad (21)$$

$$\frac{XD}{z} = 1.746 + 1.95 \frac{b}{z} + 0.0524 \frac{h}{h_0 + z - h} + 1.88 \left(Q/bz \sqrt{gd_m \left(\frac{\rho_s - \rho}{\rho} \right)} \right) - 0.534 \frac{d_{90}}{d_m} - 1.99 \frac{B}{b} \quad (22)$$

The results of MLR equations in the calibration and testing stages of the dataset are provided in Table 4. With regard to these results, it is clear that although the MLR models in the calibration stage have appropriate results, in the testing stage their results are not excellent, because of the incapability of regression techniques to learn and extract the physical background of scour phenomenon from the numerical values of the data set. In this case the best prediction of the MLR model in the testing of the data set is for XD/Z with R² = 0.88, RMSE = 0.182, MAE = 0.142, AARE = 9.74%, and TS_{100%} = 64.25, which shows that the MLR model in a best situation in 64.25% of the predictions has errors greater than 100%. Moreover, the performance of the empirical equations is assessed by evaluating the scatter plot and series plots of observed and estimated values in Figure 3. It could be inferred from Figure 3 and Table 4 where the scour depth (S/Z) is used, that the MLR mode appears as the lowest accurate estimations (R² = 0.659 and 0.462; RMSE = 0.289 and 0.192; MAE = 0.185 and 0.141; AARE(%) = 75.19 and 65.84; and TS_{100%} = 530.82 and 287.01 in training and testing steps respectively). In the case of the MLR model,

Table 6. Statistical results of the MLP model in the prediction of scour hole dimensions.

Statistical parameter						Scour parameter	Stage
NSE	TS100%	AARE (%)	MAE	RMSE	R ²		
0.99	79.3	9.325	0.018	0.03	0.9964	S/Z	Training
0.998	29.16	5.71	0.04	0.05	0.9985	XS/Z	Training
0.997	17.81	1.94	0.029	0.045	0.9974	XD/Z	Training
0.995	32.75	4.92	0.01	0.01	0.9952	Hd/Z	Training
0.83	216.57	23.774	0.068	0.106	0.828	S/Z	Testing
0.93	46.03	12.71	0.196	0.345	0.9514	XS/Z	Testing
0.96	20.91	4.66	0.07	0.095	0.9689	XD/Z	Testing
0.96	67.13	14.3	0.018	0.023	0.964	hd/Z	Testing

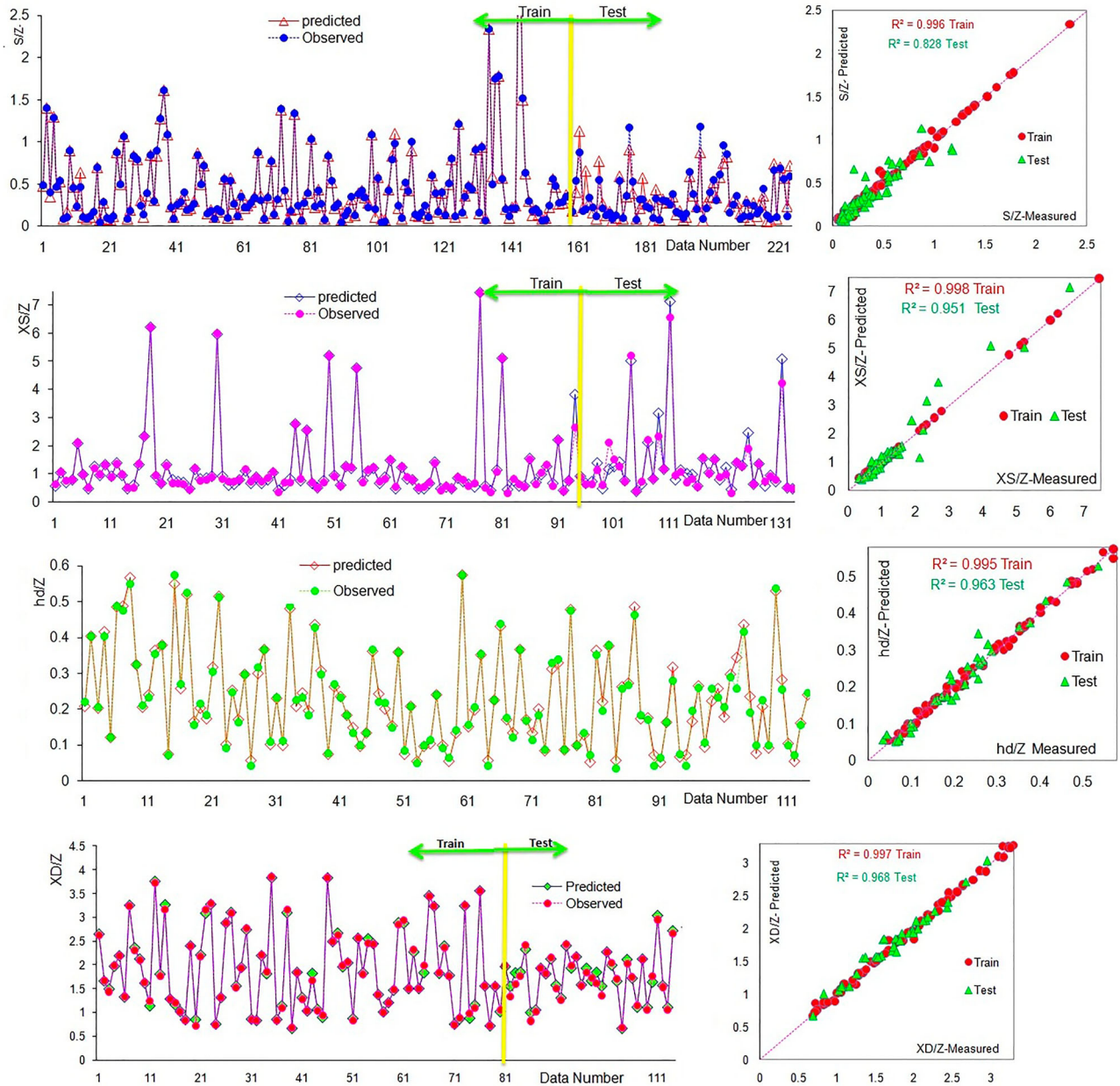


Figure 4. Comparison of the MLP model results for S/Z , XS/Z , XD/Z , and hd/Z in training and testing steps.

the most accurate estimations are derived for XD/Z as the location of the maximum deposits.

3.3. Results of MNL model

Using the collected data set, four multiple non-linear regression equations, based on the partial least square method for each scour variable established, are as follows:

$$\frac{S}{Z} = 0.539 \left(\frac{b}{z}\right)^{0.149} \left(\frac{h}{h_0 + z}\right)^{0.275} \left(\frac{b}{B}\right)^{-0.201} \left(\frac{Q}{bz\sqrt{gd_m} \left(\frac{\rho_s - \rho}{\rho}\right)}\right)^{0.264} \left(\frac{d_{90}}{d_m}\right)^{-0.802} \quad (23)$$

$$\frac{XS}{Z} = 1.841 \left(\frac{b}{z}\right)^{0.767} \left(\frac{h}{h_0 + z}\right)^{-0.152} \left(\frac{b}{B}\right)^{-0.319} \left(\frac{Q}{bz\sqrt{gd_m} \left(\frac{\rho_s - \rho}{\rho}\right)}\right)^{0.41} \left(\frac{d_{90}}{d_m}\right)^{-0.254} \quad (24)$$

$$\frac{XD}{Z} = 0.452 \left(\frac{b}{z}\right)^{0.64} \left(\frac{h}{h_0 + z}\right)^{0.0207} \left(\frac{b}{B}\right)^{-0.752} \left(\frac{Q}{bz\sqrt{gd_m} \left(\frac{\rho_s - \rho}{\rho}\right)}\right)^{0.704} \left(\frac{d_{90}}{d_m}\right)^{-0.066} \quad (25)$$

Table 7. Statistical results of the RBF model in the prediction of scour hole dimensions.

Statistical parameter						Scour parameter	Stage
NSE	TS100%	AARE (%)	MAE	RMSE	R ²		
0.89	530.54	27.63	0.0899	0.162	0.895	S/Z	Training
-0.157	122.342	43.9	0.083	0.084	0.998	XS/Z	Training
0.98	26.61	5.317	0.084	0.12	0.98	XD/Z	Training
-5.68	1025.41	211.45	0.313	0.32	0.788	hd/Z	Training
0.73	308.03	32.039	0.084	0.131	0.7608	S/Z	Testing
-0.865	102.804	52.4	0.093	0.096	0.945	XS/Z	Testing
0.94	38.87	8.97	0.096	0.13	0.945	XD/Z	Testing
-23.18	1348.8	308.82	0.46	0.54	0.3353	hd/Z	Testing

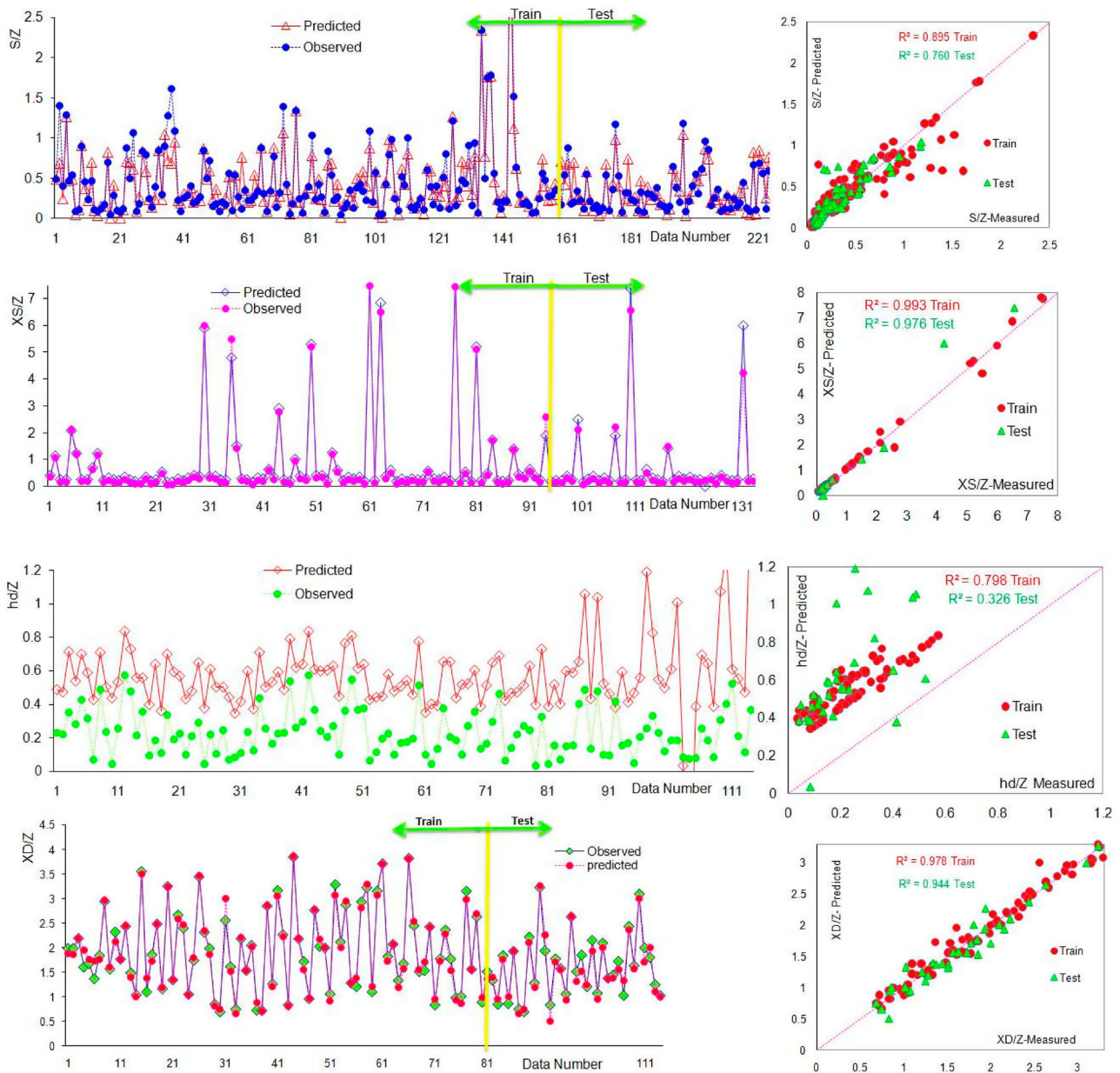


Figure 5. Comparison of the RBF model results for S/Z, XS/Z, XD/Z, and hd/Z in training and testing steps.

$$\frac{XD}{Z} = 3.328 \left(\frac{b}{z}\right)^{0.423} \left(\frac{h}{h_0 + z}\right)^{0.088} \left(\frac{b}{B}\right)^{-0.459} \left(\frac{Q}{bz\sqrt{gd_m(\frac{\rho_s - \rho}{\rho})}}\right)^{0.482} \left(\frac{d_{90}}{d_m}\right)^{-0.425} \quad (26)$$

Table 5 shows the results of the MNLN equations. In same way as with the MLR model, the MNLN model at the calibration stage has relatively proper results but at the testing stage, the error values of predictions increased. Similar with the MLR model, the best results are for

Table 8. Statistical results of the ANFIS model in the prediction of scour hole dimensions.

Statistical parameter						Scour parameter	Stage
NSE	TS100%	AARE (%)	MAE	RMSE	R ²		
0.94	219.842	25.4488	0.0753	0.125	0.9364	S/Z	Training
0.9	104.8256	7.9958	0.1266	0.4103	0.9003	XS/Z	Training
0.998	11.5458	2.2761	0.0333	0.0436	0.9975	XD/Z	Training
0.998	11.8872	2.0178	0.0035	0.0055	0.9985	hd/Z	Training
0.91	128.6585	18.7303	0.0505	0.078	0.9147	S/Z	Testing
0.461	107.7542	17.5089	0.4136	0.9302	0.5669	XS/Z	Testing
0.95	15.3488	5.0554	0.0805	0.1102	0.9558	XD/Z	Testing
0.87	101.9133	20.6725	0.0286	0.0448	0.8790	hd/Z	Testing

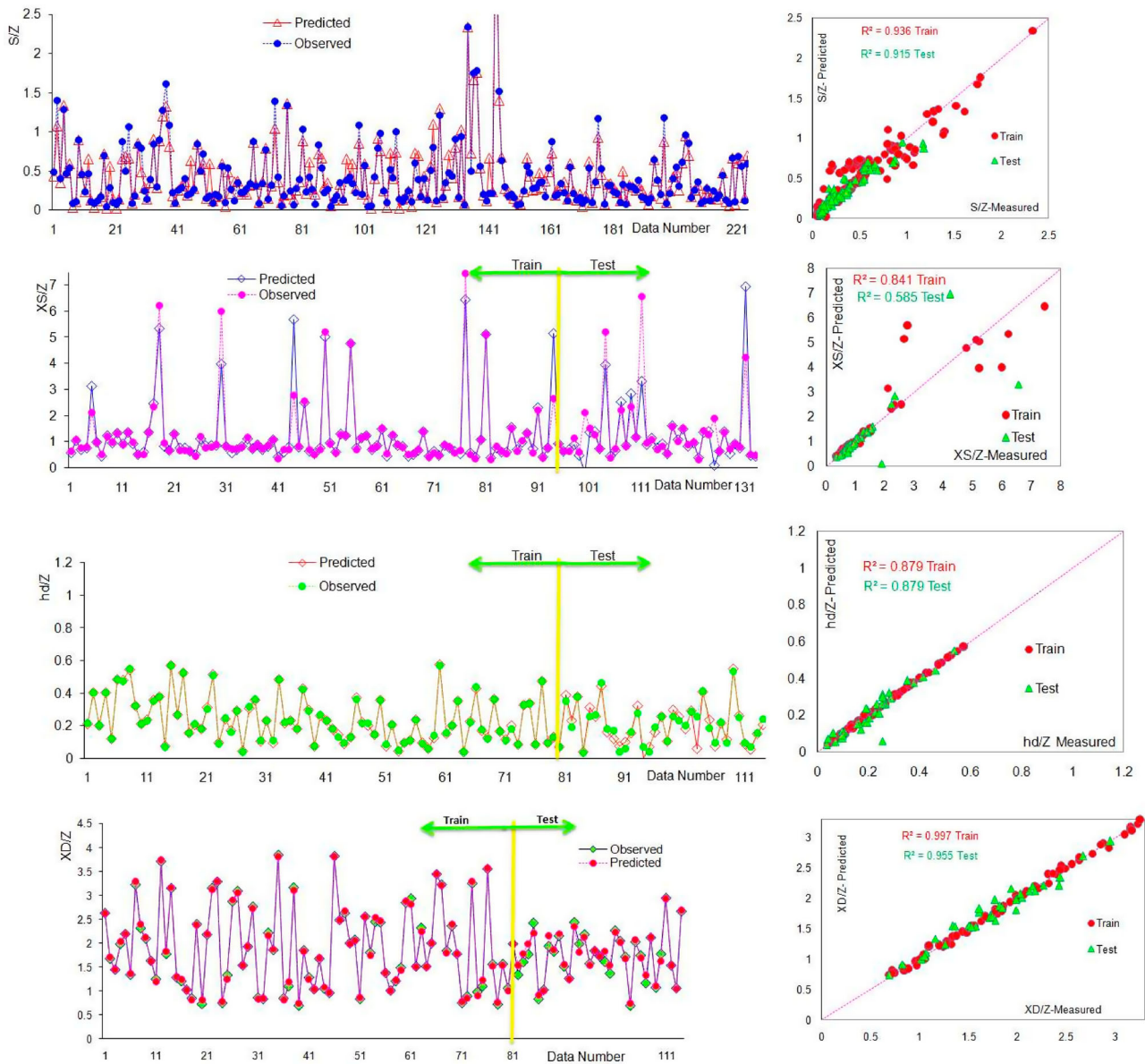


Figure 6. Comparison of the ANFIS model results for S/Z, XS/Z, XD/Z, and hd/Z in training and testing steps.

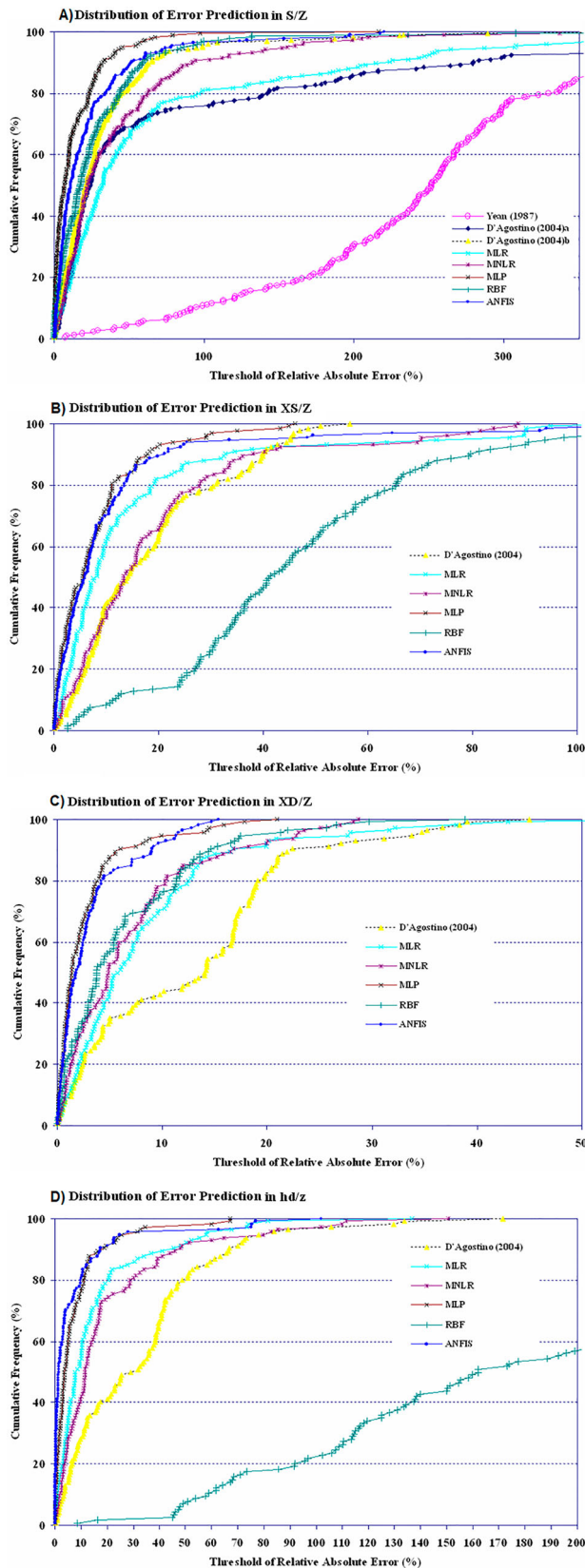


Figure 7. Error Prediction Distribution of models in (A) S/Z, (B) XS/Z, (C) XD/Z, and (D) hd/z respectively.

XD/Z with $R^2 = 0.88$, RMSE = 0.181, MAE = 0.131, AARE = 8.116, and $TS_{100\%} = 28.163$, while for the other scour hole parameters the MNLR model does not provide accurate results. That the MNLR model in best condition for XD/Z in 28.7% of the predictions have error values greater than 100% is also relatively high, but in comparison with the previous methods has better results. The scatter plot and series graphs of MLR and MNLR model results are compared in Figure 3. In regard to the results in this figure, it is concluded that the MNLR model has somewhat better predictions than the MLR.

3.4. MLP model results

Using collected field and experimental data sets the MLP model has been trained and its optimized parameters and structures are obtained using a trial and error process. The best accuracy of tested activation and transformation function in hidden layer was obtained by logsig, and for the output layer, it was obtained by purelin. The activation function in MLP model was logsig with five nodes in input layer, five and three nodes in two hidden layers respectively and one node in the output layer. The results of the MLP model in the training and testing and overall for the data set is presented in Table 6 and Figure 4. From this table it is concluded that the best results of the test data set come for XD/Z variable with $R^2 = 0.97$, RMSE = 0.095, MAE = 0.07, AARE = 4.66, and $TS_{100\%} = 20.91$. Comparison of the MLP models results in ‘

Table 6 while Tables 3–5 somewhat shows the better ability of MLP models in simulating scour dimensions downstream of grade control structures. Also, the results of the MLP model in Figure 4 declare that the MLP model has accurate estimations for S/Z, XS/Z, XD/Z, and hd/Z in training and testing steps. Regarding Figure 4 with Figure 3, the comparison between MLP, MNLR, and MLR shows the better function in MLP estimations. Relatively good estimations are derived from all MLP models including the five input parameters of individual data sets.

3.5. RBF model results

The results of the artificial neural network radial basis function model are provided in Table 7. In this table, the best results for the training of the data sets comes for XD/Z with $R^2 = 0.945$, RMSE = 0.13, MAE = 0.096, AARE = 8.97, and $TS_{100\%} = 38.87$. So the RBF model in 38.87% of the predictions have error values greater than 100% which is greater than the MLP, MNLR, and MLR models. Comparing the results in Table 7 with Table 6

shows the superiority of the MLP model over the RB model. Also, the comparison between observed and estimated values of scour geometry by RBF in Figure 5 shows that although it has acceptable predictions for S/Z, XS/Z, and XD/Z, it has major overestimations for hd/Z. This figure shows that the developed RBF model and observed data of S/Z, XS/Z, and XS/S located near the 1:1 line with a strong data correlation in training and testing stages. These R^2 values are higher than those resulting from MLR and MNLR. However, when using the RBF model for prediction of hd/Z, it demonstrates a high error, indicating the limitations of the RBF model when it is used to applied cases of scour deposition height estimations.

3.6. ANFIS model results

The results of the ANFIS model for three variables of scour hole geometry in several stages of model development are presented in Table 8 and Figure 6. In the training of the dataset the best predictions of the ANFIS model comes for the XD/Z with $R^2 = 0.96$, RMSE = 0.1102, MAE = 0.0805, AARE = 5.05%, and $TS_{100\%} = 15.3488$. The ANFIS model only in 15.3488% of predictions have errors greater than 100% and shows its ability in the prediction of scour hole length. Comparing the results of RBF, MLP, and empirical equations with the ANFIS model revealed that in all of four predictive parameters, the developed ANFIS model provided better results.

The worst results of ANFIS are for the location of the maximum scour depth (XS/Z) in the testing stage, while the best results of ANFIS are provided for the location of deposited sediments (XD/Z). After that there is S/Z and hd/Z in training and testing steps respectively (Figure 6). Overall, based on the results of models, it can be concluded that the ANFIS approach is a precise model in the simulation of scour hole geometry dimensions and it can be applied for stable design of grade control structure in alluvial channels.

3.7. Comparing all models

Developing a model with a higher scale of precision in the estimation of grade control scour is of great significance in confirming the reliability and safety of water supply devices in irrigation networks and requires selecting the best estimation model. The applicability and effectiveness of the six developed models in estimating grade control scour geometry were investigated comparatively. To investigate the performance of developed models, and figure out superior models, simultaneous assessment of models are done. For this purpose the evaluation of

model results are done using error distribution of estimations. Comparing the results of six methods based on Tables 3–8 for four variables of S/Z, XS/Z, XD/Z, and hd/z shows that: for S/Z parameter, the maximum scour depth, the best predictions come from the ANFIS model; for XS/Z the best results is from the MLP model; for XD/Z the best prediction is from the ANFIS model; and in the hd/z variable the MLP model has the best predictions. Based on the error distribution of models in Figure 7, it can be noted that the ANFIS and MLP models have estimated the scour geometry with approximately the same accuracy and their results are better than the others. This indicates that for all four scour parameters the intelligence models have superiority to the regression equations and can be used as the accurate design techniques in the design of grade control structures. Figure 7 shows the error distribution of six models on all of the prediction variables regarding all of the data set. All developed regression equations exhibit a large estimation error while the artificial intelligence models perform better due to the valuable ability to estimate scour geometry from numerical information.

The best results over training data derived for XS/Z, and hd/Z by the MLP model with R^2 , 0.95, and 0.96 respectively; the best predictions for S/Z and XD/Z are from ANFIS model with R^2 0.91 and 0.96 respectively. The results indicated that the application of MLP and ANFIS results in the accurate prediction of scour geometry for the designing of stable grade control structures in alluvial irrigation channels. The MLP and ANFIS models are information-based models that use inherent knowledge of a phenomenon to infer the physical process behind the scour formation. The MLP model adopts its weights based on the Levenberg-Marquardt training algorithm that finds the best vector of weights of model structure; the ANFIS combines fuzzy logic as a knowledge inference engine for MLP to take advantage of training and uncertainties of fuzzy membership functions.

4. Conclusions

The ability to accurately estimate the whole geometry of scour holes downstream of grade control structures is important for developing irrigation regulation structures. This study employed different methods and tools to improve existing empirical scour equations for grade control structures. In this paper the authors used six methods for predicting local scour on alluvial beds downstream of grade control structures in irrigation canals. The geometry of scour holes described by four parameters of: maximum scour depth (S); distance of S from the weir (XS); maximum height of downstream deposited

sediments (h_d); and distance of h_d from the weir. The models are: empirical equations; multi layer perceptron (MLP) neural networks; radial basis functions (RBF) neural networks; adaptive neuro fuzzy inference systems (ANFIS); multiple linear regression (MLR); and multiple non-linear regression (MNLR). Based on the results of the study and statistical parameters and indexes it is concluded that the intelligence methods of MLP and ANFIS have more accurate predictions than RBF, MNLR, MLR, and previous equations and that the newly developed models in this comparative study can be used as design methods for grade control structures. Existing studies and models, which are studied in the literature, were applicable for the estimation of only one dimension of scour geometry, while in the present study the newly developed models that are explored here were developed to estimate different dimensions of scour geometry. This led to the improvements of scour hole studies from a single parameter to a geometry space. Nevertheless, further investigations are required to improve the uncertainty of the developed methods. With all the results of models considered, this paper concludes that soft computing models are superior to the classical models, but they are black box models and do not provide explicit equations for scour hole prediction. Further studies are required to derive explicit predictive equations based on ANFIS, MLP, and RBF manipulation that can be used in application design; uncertainty analysis of prediction results also remains another improvement for future studies. Future studies also could use comparative analysis between the results from other soft computing models such as SVM, GEP, and LEM methods with the results of the developed models in the present paper. as well as with a combination of ANFIS and ANN models with meta heuristic optimization algorithms as the training algorithm could be an another field for next studies.

Disclosure statement

No potential conflict of interest was reported by the authors.

Funding

This work was supported by the Ministry of Higher Education under Skim Geran Penyelidikan Fundamental (FRGS) (grant number FRGS/1/2018/ICT04/UKM/02/8).

References

- ASCE Task Committee. (2000). Artificial neural networks in Hydrology. I: Preliminary concepts. *Journal of Hydrologic Engineering*, 5(2), 124–137. doi:10.1061/(ASCE)1084-0699(2000)5:2(115)
- Azamathulla, H. M. (2005). *Neural networks to estimate scour downstream of ski-jump bucket spillway [D]* (Doctoral dissertation, Ph. D. Thesis). Indian Institute of Technology, Bombay.
- Azamathulla, H. M. (2012). Gene expression programming for prediction of scour depth downstream of sills. *Journal of Hydrology*, 460–461, 156–159. doi:10.1016/j.jhydrol.2012.06.034
- Bateni, S. M., & Jeng, D. S. (2007). Estimation of pile group scour using adaptive neuro-fuzzy approach. *Ocean Engineering*, 34(8–9), 1344–1354. doi:10.1016/j.oceaneng.2006.07.003
- Chang, C. K., Azamathulla, H. M., Zakaria, N. A., & Ab Ghani, A. (2012). Appraisal of soft computing techniques in prediction of total bed material load in tropical rivers. *Journal of Earth System Science*, 121(1), 125–133. doi:10.1007/s12040-012-0138-1
- Chinnarasri, C., & Kositgittiwong, D. (2008, October). Laboratory study of maximum scour depth downstream of sills. *Proceedings of the Institution of Civil Engineers - Water Management*, 161(5), 267–275. Thomas Telford Ltd.
- Chau, K. W. (2017). Use of meta-heuristic techniques in rainfall-runoff modelling. *Water*, 9(3), 186. doi:10.3390/w9030186
- Choubin, B., Malekian, A., Samadi, S., Khalighi-Sigaroodi, S., & Sajedi-Hosseini, F. (2017). An ensemble forecast of semi-arid rainfall using large-scale climate predictors. *Meteorological Applications*, 24(3), 376–386.
- D'Agostino, V. (1994). Indagine sullo scavo a valle di opera trasversali mediante modellofisico a fondo mobile. *L'Energia Elettrica* 71(2), 37–51 (in Italian).
- D'Agostino, V., & Ferro, V. (2004). Scour on alluvial bed downstream of grade-control structures. *Journal of Hydraulic Engineering*, 130(1), 24–37. doi:10.1061/(ASCE)0733-9429(2004)130:1(24)
- Dehghani, M., Riahi-Madvar, H., Hooshyaripor, F., Mosavi, A., Shams Shirband, S., Zavadskas, E. K., & Chau, K. W. (2019). Prediction of hydropower generation using grey wolf optimization adaptive neuro-fuzzy inference system. *Energies*, 12(2), 289.
- Dehghani, M., Saghafian, B., Nasiri Saleh, F., Farokhnia, A., & Noori, R. (2014). Uncertainty analysis of streamflow drought forecast using artificial neural networks and Monte-Carlo simulation. *International Journal of Climatology*, 34, 1169–1180. doi:10.1002/joc.3754
- Elnikhely, E. A. (2018). Investigation and analysis of scour downstream of a spillway. *Ain Shams Engineering Journal*, 9(4), 2275–2282.
- Falciai, M., & Giacomini, A. (1978). Indagine Sui Gorgi Che Si Formano a Valle Delle Traverse Torrentizie. *Italia Forestale Montana*, 23(3), 111–123. (in Italian).
- Gaudio, R., Marion, A., & Bovolín, V. (2000). Morphological effects of bed sills in degrading rivers. *Journal of Hydraulic Research*, 38(2), 89–96. doi:10.1080/00221680009498344
- Goel, A., & Pal, M. (2009). Application of support vector machines in scour prediction on grade-control structures. *Engineering Applications of Artificial Intelligence*, 22(2), 216–223. doi:10.1016/j.engappai.2008.05.008
- Guan, D., Melville, B., & Friedrich, H. (2016). Local scour at submerged weirs in sand-bed channels. *Journal of Hydraulic Research*, 54(2), 172–184. doi:10.1080/00221686.2015.1132275
- Ham, M. F., & Kostanic, I. (2001). *Principles of neuro computing for Science and Engineering*. New York: McGraw-Hill.
- Hameed, M., Sharqi, S. S., Yaseen, Z. M., Afan, H. A., Hussain,

- A., & Elshafie, A. (2017). Application of artificial intelligence (AI) techniques in water quality index prediction: A case study in tropical region, Malaysia. *Neural Computing and Applications*, 28(1), 893–905.
- Hoffmans, G. J. C. M., & Verheij, H. J. (1997). *Scour Manual* (Vol. 96). Rotterdam: A.A. Balkema. CRC Press.
- Hooshyaripor, F., Tahershamsi, A., & Golian, S. (2014). Application of copula method and neural networks for predicting peak outflow from breached embankments. *Journal of Hydro-Environment Research*, 8(3), 292–303. doi:10.1016/j.jher.2013.11.004
- Jang, J. S. R., & Gulley, N. (1995). *The fuzzy logic Toolbox for Use with MATLAB*. Natick, MA: The Mathworks Inc.
- Juahir, H., Zain, S. M., Aris, A. Z., Yusoff, M. K., & Mokhtar, M. B. (2010). Spatial assessment of Langat river water quality using chemometrics. *Journal of Environmental Monitoring*, 12(1), 287–295.
- Karbasi, M., & Azamathulla, H. M. (2017). Prediction of scour caused by 2D horizontal jets using soft computing techniques. *Ain Shams Engineering Journal*, 8(4), 559–570. doi:10.1016/j.asej.2016.04.001
- Khadangi, E., Madvar, H. R., & Ebadzadeh, M. M. (2009). Comparison of ANFIS and RBF models in daily stream flow forecasting. In *2009 2nd International Conference on Computer, control and Communication* (pp. 1–6). IEEE.
- Khan, M., Azamathulla, H. M. D., & Tufail, M. (2012). Gene-expression programming to predict pier scour depth using laboratory data. *Journal of Hydroinformatics*, 14, 628–645. doi:10.2166/hydro.2011.008
- Kisi, O., & Cobaner, M. (2009). Modeling River stage-discharge Relationships using different neural network computing techniques. *CLEAN - Soil, Air, Water*, 37(2), 160–169.
- Kumar, C., & Sreeja, P. (2012). Evaluation of selected equations for predicting scour at downstream of ski-jump spillway using laboratory and field data. *Engineering Geology*, 129–130, 98–103. doi:10.1016/j.enggeo.2012.01.014
- Laucelli, D., & Giustolisi, O. (2011). Scour depth modelling by a multi-objective evolutionary paradigm. *Environmental Modelling & Software*, 26(4), 498–509. doi:10.1016/j.envsoft.2010.10.013
- Lenzi, M. A., Marion, A., & Comiti, F. (2003). Local scouring at grade-control structures in alluvial mountain rivers. *Water Resources Research*, 39(7), doi:10.1029/2002WR001815
- Lenzi, M.A., Marion, A., Comiti, F., & Gaudio, R. (2000). Riduzione Dello Scavo a Valle di Soglie Di Fondo Per Effetto Dell'interferenza Tra le Opere. *Proc., 27th Convegno di Idraulica e Costruzioni Idrauliche, Genova*, 3, 271–278. (in Italian).
- Lenzi, M. A., Marion, A., Comiti, F., & Gaudio, R. (2002). Local scouring in low and high gradient streams at bed sills. *Journal of Hydraulic Research*, 40(6), 731–739. doi:10.1080/00221680209499919
- Liriano, S. L., & Day, R. A. (2001). Prediction of scour depth at culvert outlets using neural networks. *Journal of Hydroinformatics*, 3(4), 231–238. doi:10.2166/hydro.2001.0021
- Lu, J. Y., Hong, J. H., Chang, K. P., & Lu, T. F. (2013). Evolution of scouring process downstream of grade-control structures under steady and unsteady flows. *Hydrological Processes*, 27(19), 2699–2709. doi:10.1002/hyp.9318
- Marion, A., Tregnaghi, M., & Tait, S. (2006). Sediment supply and local scouring at bed sills in high-gradient streams. *Water Resources Research*, 42(6), doi:10.1029/2005WR004124
- Mason, P. J., & Arumugam, K. (1985). Free Jet scour Below Dams and Flip Buckets. *Journal of Hydraulic Engineering*, 111, 220–235. doi:10.1061/(ASCE)0733-9429(1985)111:2(220)
- Melville, B. W., & Lim, S. Y. (2014). Scour caused by 2D horizontal jets. *Journal of Hydraulic Engineering*, 140(2), 149–155. doi:10.1061/(ASCE)HY.1943-7900.0000807
- Moazenzadeh, R., Mohammadi, B., Shamshirband, S., & Chau, K. W. (2018). Coupling a firefly algorithm with support vector regression to predict evaporation in northern Iran. *Engineering Applications of Computational Fluid Mechanics*, 12(1), 584–597.
- Mohammadpour, R. (2017). Prediction of local scour around complex piers using GEP and M5-Tree. *Arabian Journal of Geosciences*, 10(18), 416. doi:10.1007/s12517-017-3203-x
- Mossa, M. (1998). Experimental study on the scour downstream of grade-control structures. *Proc., 26th Convegno di Idraulica e Costruzioni Idrauliche, Catania*, 3, 581–594.
- Najafzadeh, M. (2015). Neuro-fuzzy GMDH based particle swarm optimization for prediction of scour depth at downstream of grade control structures. *Engineering Science and Technology, an International Journal*, 18(1), 42–51. doi:10.1016/j.jestch.2014.09.002
- Najafzadeh, M., Saberi-Movahed, F., & Sarkamaryan, S. (2018). NF-GMDH-Based self-organized systems to predict bridge pier scour depth under debris flow effects. *Marine Georesources & Geotechnology*, 36, 589–602. doi:10.1080/1064119X.2017.1355944
- Najah, A., El-Shafie, A., Karim, O. A., & El-Shafie, A. H. (2013). Application of artificial neural networks for water quality prediction. *Neural Computing and Applications*, 22(1), 187–201.
- Nguyen, T. H. T., Ahn, J., & Park, S. W. (2018). Numerical and physical investigation of the performance of Turbulence modeling Schemes around a scour hole downstream of a Fixed Bed Protection. *Water*, 10(2), 103. doi:10.3390/w10020103
- Pagliara, S. (2007). Influence of sediment gradation on scour downstream of block ramps. *Journal of Hydraulic Engineering*, 133(11), 1241–1248. doi:10.1061/(ASCE)0733-9429(2007)133:11(1241)
- Pagliara, S., & Kurdistani, S. M. (2013). Scour downstream of cross-vane structures. *Journal of Hydro-Environment Research*, 7(4), 236–242. doi:10.1016/j.jher.2013.02.002
- Pandey, M., Zakwan, M., Sharma, P. K., & Ahmad, Z. (2019). Multiple linear regression and genetic algorithm approaches to predict temporal scour depth near circular pier in non-cohesive sediment. *ISH Journal of Hydraulic Engineering*, 1–8. doi:10.1080/09715010.2018.1457455
- Rafeei-Sardooi, E., Mohseni-Saravi, M., Barkhori, S., Azareh, A., Choubin, B., & Jafari-Shalamzar, M. (2018). Drought modeling: A comparative study between time series and neuro-fuzzy approaches. *Arabian Journal of Geosciences*, 11(17), 487.
- Rajaei, A., Esmaeili Varaki, M., & Shafei Sabet, B. (2019). Experimental investigation on local scour at the downstream of grade control structures with labyrinth planform. *ISH Journal of Hydraulic Engineering*, 1–11. doi:10.1080/09715010.2018.1502627

- Ramamurthy, A. S., Qu, J., & Vo, D. (2006). Nonlinear PLS method for side weir flows. *Journal of Irrigation and Drainage Engineering*, 132(5), 486–489. doi:10.1061/(ASCE)0733-9437(2006)132:5(486)
- Riahi-Madvar, H., & Seifi, A. (2018). Uncertainty analysis in bed load transport prediction of gravel bed rivers by ANN and ANFIS. *Arabian Journal of Geosciences*, 11(21), 688. doi:10.1007/s12517-018-3968-6
- Salmasi, F., Yıldırım, G., Masoodi, A., & Parsamehr, P. (2013). Predicting discharge coefficient of compound broad-crested weir by using genetic programming (GP) and artificial neural network (ANN) techniques. *Arabian Journal of Geosciences*, 6(7), 2709–2717. doi:10.1007/s12517-012-0540-7
- Sanikhani, H., Deo, R. C., Samui, P., Kisi, O., Mert, C., Mirabasi, R., . . . Yaseen, Z. M. (2018). Survey of different data-intelligent modeling strategies for forecasting air temperature using geographic information as model predictors. *Computers and Electronics in Agriculture*, 152, 242–260.
- Sanikhani, H., Kisi, O., Kiafar, H., & Ghavidel, S. Z. Z. (2015). Comparison of different data-driven approaches for modeling lake level fluctuations: The case of Manyas and Tuz Lakes (Turkey). *Water Resources Management*, 29(5), 1557–1574.
- Scimemi, E. (1939). Sulla relazione che intercede fra gli scavi osservati nelle opere idrauliche originali e nei modelli. *Energia Elettrotecnica*, 16(11), 3–8.
- Sarkar, A., & Dey, S. (2004). Review on local scour due to jets. *Int. J. Sediment Res*, 19(3), 210–238.
- Scurlock, S. M., Thornton, C. I., & Abt, S. R. (2012). Equilibrium scour downstream of three-dimensional grade-control structures. *Journal of Hydraulic Engineering*, 138(2), 167–176. doi:10.1061/(ASCE)HY.1943-7900.0000493
- Seifi, A., & Riahi, H. (2018). Estimating daily reference evapotranspiration using hybrid gamma test-least square support vector machine, gamma test-ANN, and gamma test-ANFIS models in an arid area of Iran. *Journal of Water and Climate Change*. doi:10.2166/wcc.2018.003
- Seifi, A., & Riahi-Madvar, H. (2019). Improving one-dimensional pollution dispersion modeling in rivers using ANFIS and ANN-based GA optimized models. *Environmental Science and Pollution Research*, 26(1), 867–885. doi:10.1007/s11356-018-3613-7
- Sui, J., Faruque, M. A. A., & Balachandar, R. (2008). Influence of channel width and tailwater depth on local scour caused by square jets. *Journal of Hydro-Environment Research*, 2, 39–45. doi:10.1016/j.jher.2008.05.001
- Taormina, R., Chau, K. W., & Sivakumar, B. (2015). Neural network river forecasting through baseflow separation and binary-coded swarm optimization. *Journal of Hydrology*, 529, 1788–1797.
- Termini, D., & Sammartano, V. (2012). Morphodynamic processes downstream of man-made structural interventions: Experimental investigation of the role of turbulent flow structures in the prediction of scour downstream of a rigid bed. *Physics and Chemistry of the Earth, Parts A/B/C*, 49, 18–31. doi:10.1016/j.pce.2011.12.006
- Veronese, A. (1937). Erosioni di fondo a valle di un scarico. *Annali dei Lavori Pubblici*, 75(9), 717–726 (in Italian).
- Wan Mohtar, W. H. M., Afan, H., El-Shafie, A., Bong, C. H. J., & Ab. Ghani, A. (2018). Influence of bed deposit in the prediction of incipient sediment motion in sewers using artificial neural networks. *Urban Water Journal*, 15(4), 296–302.
- Wu, C. L., & Chau, K. W. (2011). Rainfall–runoff modeling using artificial neural network coupled with singular spectrum analysis. *Journal of Hydrology*, 399(3–4), 394–409.
- Yaseen, Z. M., El-Shafie, A., Afan, H. A., Hameed, M., Mohtar, W. H. M. W., & Hussain, A. (2016). RBFNN versus FFNN for daily river flow forecasting at Johor River, Malaysia. *Neural Computing and Applications*, 27(6), 1533–1542.
- Yaseen, Z. M., Sulaiman, S. O., Deo, R. C., & Chau, K. W. (2019). An enhanced extreme learning machine model for river flow forecasting: State-of-the-art, practical applications in water resource engineering area and future research direction. *Journal of Hydrology*, 569, 387–408.
- Zadeh, L. A. (1965). Fuzzy sets. *Information and Control*, 8(3), 338–353.
- Zounemat-Kermani, M., Beheshti, A. A., Ataie-Ashtiani, B., & Sabbagh-Yazdi, S. R. (2009). Estimation of current-induced scour depth around pile groups using neural network and adaptive neuro-fuzzy inference system. *Applied Soft Computing*, 9(2), 746–755. doi:10.1016/j.asoc.2008.09.006

Appendix 1: The raw data set used in the present study.

Number	Z(m)	Ho(m)	H(m)	Q/B	s(m)	xs	hd	XD	d ₅₀	B	d ₉₀
1	0.71	0.044	0.083	0.0167	0.057	0.24	0.03	0.49	0.0041	0.5	0.007
2	0.71	0.044	0.086	0.0167	0.06	0.24	0.03	0.49	0.0041	0.5	0.007
3	0.71	0.044	0.191	0.0167	0.065	0.255	0.05	0.51	0.0041	0.5	0.007
4	0.71	0.044	0.239	0.0167	0.086	0.26	0.06	0.53	0.0041	0.5	0.007
5	0.71	0.044	0.244	0.0167	0.09	0.265	0.055	0.53	0.0041	0.5	0.007
6	0.71	0.044	0.326	0.0167	0.09	0.285	0.07	0.59	0.0041	0.5	0.007
7	0.71	0.071	0.103	0.0333	0.085	0.35	0.065	0.715	0.0041	0.5	0.007
8	0.71	0.071	0.119	0.0333	0.083	0.395	0.078	0.75	0.0041	0.5	0.007
9	0.71	0.071	0.211	0.0333	0.095	0.43	0.065	0.725	0.0041	0.5	0.007
10	0.71	0.071	0.349	0.0333	0.105	0.355	0.07	0.75	0.0041	0.5	0.007
11	0.71	0.071	0.385	0.0333	0.095	0.37	0.08	0.76	0.0041	0.5	0.007
12	0.71	0.093	0.228	0.05	0.116	0.47	0.085	0.91	0.0041	0.5	0.007
13	0.71	0.093	0.274	0.05	0.111	0.525	0.1	0.945	0.0041	0.5	0.007
14	0.71	0.093	0.365	0.05	0.125	0.52	0.08	0.895	0.0041	0.5	0.007
15	0.71	0.093	0.4	0.05	0.12	0.42	0.095	0.91	0.0041	0.5	0.007
16	0.71	0.113	0.208	0.0667	0.115	0.46	0.125	1.075	0.0041	0.5	0.007
17	0.71	0.113	0.241	0.0667	0.145	0.49	0.115	1.075	0.0041	0.5	0.007
18	0.71	0.113	0.325	0.0667	0.13	0.445	0.12	1.025	0.0041	0.5	0.007
19	0.71	0.113	0.38	0.0667	0.13	0.505	0.11	1.055	0.0041	0.5	0.007
20	0.71	0.131	0.255	0.0833	0.145	0.515	0.16	1.225	0.0041	0.5	0.007
21	0.71	0.131	0.276	0.0833	0.175	0.475	0.16	1.19	0.0041	0.5	0.007
22	0.71	0.131	0.307	0.0833	0.16	0.52	0.15	1.22	0.0041	0.5	0.007
23	0.71	0.131	0.36	0.0833	0.17	0.465	0.152	1.26	0.0041	0.5	0.007
24	0.71	0.131	0.4	0.0833	0.175	0.515	0.145	1.16	0.0041	0.5	0.007
25	0.71	0.146	0.319	0.1	0.156	0.575	0.165	1.32	0.0041	0.5	0.007
26	0.71	0.146	0.322	0.1	0.165	0.565	0.17	1.295	0.0041	0.5	0.007
27	0.71	0.146	0.354	0.1	0.155	0.54	0.135	1.26	0.0041	0.5	0.007
28	0.71	0.146	0.41	0.1	0.185	0.505	0.16	1.26	0.0041	0.5	0.007
29	0.71	0.162	0.33	0.1167	0.195	0.58	0.19	1.41	0.0041	0.5	0.007
30	0.71	0.162	0.37	0.1167	0.203	0.57	0.185	1.41	0.0041	0.5	0.007
31	0.71	0.162	0.425	0.1167	0.195	0.56	0.175	1.37	0.0041	0.5	0.007
32	0.71	0.176	0.337	0.1333	0.19	0.625	0.21	1.53	0.0041	0.5	0.007
33	0.71	0.176	0.38	0.1333	0.21	0.58	0.21	1.49	0.0041	0.5	0.007
34	0.71	0.176	0.38	0.1333	0.215	0.54	0.205	1.505	0.0041	0.5	0.007
35	0.71	0.176	0.435	0.1333	0.205	0.63	0.18	1.44	0.0041	0.5	0.007
36	0.71	0.19	0.4	0.15	0.255	0.635	0.24	1.65	0.0041	0.5	0.007
37	0.71	0.19	0.415	0.15	0.24	0.64	0.23	1.61	0.0041	0.5	0.007
38	0.71	0.205	0.42	0.1667	0.28	0.7	0.25	1.68	0.0041	0.5	0.007
39	0.71	0.205	0.435	0.1667	0.285	0.705	0.255	1.705	0.0041	0.5	0.007
40	0.41	0.043	0.105	0.0167	0.065	0.215	0.045	0.43	0.0041	0.5	0.007
41	0.41	0.043	0.332	0.0167	0.09	0.265	0.055	0.55	0.0041	0.5	0.007
42	0.41	0.07	0.104	0.0333	0.102	0.3	0.075	0.64	0.0041	0.5	0.007
43	0.41	0.07	0.123	0.0333	0.1	0.3	0.075	0.63	0.0041	0.5	0.007
44	0.41	0.07	0.159	0.0333	0.11	0.32	0.07	0.645	0.0041	0.5	0.007
45	0.41	0.07	0.353	0.0333	0.14	0.37	0.075	0.755	0.0041	0.5	0.007
46	0.41	0.091	0.174	0.05	0.13	0.35	0.1	0.82	0.0041	0.5	0.007
47	0.41	0.091	0.23	0.05	0.145	0.37	0.09	0.84	0.0041	0.5	0.007
48	0.41	0.091	0.284	0.05	0.15	0.345	0.095	0.85	0.0041	0.5	0.007
49	0.41	0.091	0.365	0.05	0.165	0.44	0.095	0.9	0.0041	0.5	0.007
50	0.41	0.091	0.37	0.05	0.155	0.42	0.11	0.895	0.0041	0.5	0.007
51	0.41	0.091	0.4	0.05	0.14	0.51	0.095	0.995	0.0041	0.5	0.007
52	0.41	0.11	0.244	0.0667	0.145	0.4	0.13	0.95	0.0041	0.5	0.007
53	0.41	0.11	0.378	0.0667	0.175	0.49	0.115	1.005	0.0041	0.5	0.007
54	0.41	0.128	0.255	0.0833	0.165	0.445	0.15	1.095	0.0041	0.5	0.007
55	0.41	0.128	0.286	0.0833	0.195	0.44	0.145	1.135	0.0041	0.5	0.007
56	0.41	0.128	0.39	0.0833	0.2	0.55	0.155	1.205	0.0041	0.5	0.007
57	0.41	0.145	0.288	0.1	0.185	0.485	0.18	1.21	0.0041	0.5	0.007
58	0.41	0.145	0.38	0.1	0.225	0.52	0.17	1.27	0.0041	0.5	0.007
59	0.41	0.16	0.33	0.1167	0.23	0.535	0.195	1.325	0.0041	0.5	0.007
60	0.41	0.16	0.365	0.1167	0.21	0.52	0.2	1.335	0.0041	0.5	0.007
61	0.41	0.16	0.415	0.1167	0.223	0.62	0.195	1.325	0.0041	0.5	0.007
62	0.41	0.174	0.349	0.1333	0.22	0.56	0.22	1.415	0.0041	0.5	0.007
63	0.41	0.174	0.405	0.1333	0.235	0.63	0.21	1.46	0.0041	0.5	0.007
64	0.41	0.188	0.395	0.15	0.25	0.625	0.235	1.525	0.0041	0.5	0.007
65	0.41	0.201	0.405	0.1667	0.265	0.62	0.235	1.57	0.0041	0.5	0.007
66	0.41	0.201	0.42	0.1667	0.26	0.65	0.225	1.58	0.0041	0.5	0.007
67	0.71	0.069	0.106	0.0333	0.06	0.305	0.03	0.515	0.0041	0.5	0.007
68	0.71	0.069	0.298	0.0333	0.11	0.33	0.045	0.59	0.0041	0.5	0.007

(continued)

Appendix 1. Continued

Number	Z(m)	Ho(m)	H(m)	Q/B	s(m)	xs	hd	XD	d ₅₀	B	d ₉₀
69	0.71	0.11	0.179	0.0667	0.115	0.39	0.07	0.78	0.0041	0.5	0.007
70	0.71	0.11	0.317	0.0667	0.135	0.42	0.075	0.78	0.0041	0.5	0.007
71	0.71	0.146	0.195	0.1	0.14	0.41	0.115	0.95	0.0041	0.5	0.007
72	0.71	0.146	0.334	0.1	0.15	0.485	0.105	0.97	0.0041	0.5	0.007
73	0.71	0.175	0.242	0.1333	0.185	0.49	0.13	1.145	0.0041	0.5	0.007
74	0.71	0.175	0.35	0.1333	0.17	0.565	0.13	1.14	0.0041	0.5	0.007
75	0.71	0.203	0.375	0.1667	0.22	0.595	0.145	1.19	0.0041	0.5	0.007
76	0.71	0.071	0.086	0.0333	0.06	0.375	0.025	0.6	0.0041	0.5	0.007
77	0.71	0.071	0.138	0.0333	0.065	0.37	0.03	0.6	0.0041	0.5	0.007
78	0.71	0.071	0.192	0.0333	0.078	0.35	0.035	0.61	0.0041	0.5	0.007
79	0.71	0.071	0.244	0.0333	0.085	0.375	0.05	0.63	0.0041	0.5	0.007
80	0.71	0.071	0.33	0.0333	0.1	0.385	0.05	0.695	0.0041	0.5	0.007
81	0.71	0.071	0.412	0.0333	0.114	0.39	0.045	0.68	0.0041	0.5	0.007
82	0.71	0.112	0.158	0.0667	0.085	0.455	0.07	0.885	0.0041	0.5	0.007
83	0.71	0.112	0.35	0.0667	0.132	0.45	0.07	0.855	0.0041	0.5	0.007
84	0.71	0.148	0.228	0.1	0.15	0.515	0.11	1.11	0.0041	0.5	0.007
85	0.71	0.148	0.365	0.1	0.15	0.49	0.11	1.09	0.0041	0.5	0.007
86	0.71	0.179	0.244	0.13333	0.195	0.58	0.155	1.315	0.0041	0.5	0.007
87	0.71	0.179	0.385	0.1333	0.175	0.64	0.145	1.28	0.0041	0.5	0.007
88	0.71	0.206	0.307	0.1667	0.225	0.67	0.165	1.42	0.0041	0.5	0.0176
89	0.41	0.043	0.136	0.0167	0.045	0.215	0.04	0.34	0.0115	0.5	0.0176
90	0.41	0.043	0.331	0.0167	0.045	0.235	0.035	0.425	0.0115	0.5	0.0176
91	0.41	0.07	0.155	0.0333	0.06	0.265	0.055	0.495	0.0115	0.5	0.0176
92	0.41	0.07	0.355	0.0333	0.085	0.325	0.05	0.565	0.0115	0.5	0.0176
93	0.41	0.091	0.169	0.05	0.09	0.28	0.09	0.62	0.0115	0.5	0.0176
94	0.41	0.091	0.365	0.05	0.1	0.39	0.08	0.715	0.0115	0.5	0.0176
95	0.41	0.11	0.208	0.06667	0.105	0.34	0.11	0.755	0.0115	0.5	0.0176
96	0.41	0.11	0.351	0.06667	0.124	0.4	0.105	0.815	0.0115	0.5	0.0176
97	0.41	0.128	0.221	0.0833	0.15	0.385	0.125	0.91	0.0115	0.5	0.0176
98	0.41	0.128	0.36	0.0833	0.145	0.45	0.105	0.895	0.0115	0.5	0.0176
99	0.41	0.145	0.232	0.1	0.155	0.425	0.15	1	0.0115	0.5	0.0176
100	0.41	0.145	0.353	0.1	0.16	0.465	0.135	1	0.0115	0.5	0.0176
101	0.41	0.16	0.276	0.1167	0.172	0.48	0.165	1.08	0.0115	0.5	0.0176
102	0.41	0.16	0.36	0.1167	0.17	0.515	0.145	1.08	0.0115	0.5	0.0176
103	0.41	0.17	0.309	0.1333	0.18	0.51	0.175	1.17	0.0115	0.5	0.0176
104	0.41	0.17	0.38	0.1333	0.175	0.545	0.155	1.18	0.0115	0.5	0.0176
105	0.41	0.185	0.319	0.15	0.215	0.525	0.2	1.3	0.0115	0.5	0.0176
106	0.41	0.185	0.39	0.15	0.19	0.58	0.165	1.295	0.0115	0.5	0.0176
107	0.41	0.196	0.335	0.1667	0.22	0.565	0.215	1.35	0.0115	0.5	0.0176
108	0.41	0.196	0.375	0.1667	0.203	0.575	0.19	1.295	0.0115	0.5	0.0176
109	0.41	0.069	0.104	0.0333	0.055	0.285	0.03	0.42	0.0115	0.5	0.0176
110	0.41	0.069	0.301	0.0333	0.085	0.29	0.035	0.477	0.0115	0.5	0.0176
111	0.41	0.145	0.136	0.1	0.094	0.385	0.08	0.725	0.0115	0.5	0.0176
112	0.41	0.145	0.334	0.1	0.11	0.49	0.085	0.795	0.0115	0.5	0.0176
113	0.41	0.203	0.195	0.1667	0.165	0.475	0.15	1.02	0.0115	0.5	0.0176
114	0.41	0.203	0.36	0.1667	0.135	0.565	0.105	1.05	0.0115	0.5	0.0176
115	1.025	0.075	0.1	0.0374	0.065	NA	NA	NA	0.0362	0.5	0.0362
116	1.053	0.092	0.145	0.0516	0.06	NA	NA	NA	0.0362	0.5	0.0362
117	1.056	0.104	0.16	0.062	0.07	NA	NA	NA	0.0362	0.5	0.0362
118	1.072	0.118	0.19	0.0744	0.08	NA	NA	NA	0.0362	0.5	0.0362
119	1.134	0.081	0.215	0.042	0.06	NA	NA	NA	0.0362	0.5	0.0362
120	1.144	0.071	0.215	0.035	0.085	NA	NA	NA	0.0362	0.5	0.0362
121	1.118	0.107	0.225	0.0646	0.1	NA	NA	NA	0.0362	0.5	0.0362
122	1.118	0.117	0.235	0.074	0.11	NA	NA	NA	0.0362	0.5	0.0362
123	1.106	0.127	0.233	0.0828	0.12	NA	NA	NA	0.0362	0.5	0.0362
124	1.146	0.064	0.21	0.03	0.055	NA	NA	NA	0.021	0.5	0.021
125	1.133	0.087	0.22	0.0472	0.1	NA	NA	NA	0.021	0.5	0.021
126	1.138	0.102	0.24	0.0596	0.105	NA	NA	NA	0.021	0.5	0.021
127	1.141	0.109	0.25	0.0658	0.11	NA	NA	NA	0.021	0.5	0.021
128	1.136	0.114	0.25	0.0711	0.12	NA	NA	NA	0.021	0.5	0.021
129	1.04	0.052	0.092	0.0216	0.05	NA	NA	NA	0.021	0.5	0.021
130	1.057	0.073	0.13	0.0364	0.065	NA	NA	NA	0.021	0.5	0.021
131	1.048	0.087	0.135	0.0474	0.08	NA	NA	NA	0.021	0.5	0.021
132	1.061	0.099	0.16	0.057	0.09	NA	NA	NA	0.021	0.5	0.021
133	1.032	0.108	0.14	0.065	0.12	NA	NA	NA	0.021	0.5	0.021
134	1.022	0.118	0.14	0.0746	0.14	NA	NA	NA	0.021	0.5	0.021
135	1.112	0.053	0.165	0.0224	0.055	NA	NA	NA	0.0142	0.5	0.0142
136	1.11	0.075	0.185	0.0376	0.095	NA	NA	NA	0.0142	0.5	0.0142
137	1.108	0.092	0.2	0.0512	0.11	NA	NA	NA	0.0142	0.5	0.0142

(continued)

Appendix 1. Continued

Number	Z(m)	Ho(m)	H(m)	Q/B	s(m)	xs	hd	XD	d ₅₀	B	d ₉₀
138	1.143	0.107	0.25	0.0646	0.11	NA	NA	NA	0.0142	0.5	0.0142
139	1.014	0.036	0.05	0.0123	0.08	NA	NA	NA	0.0142	0.5	0.0142
140	1.018	0.052	0.07	0.0221	0.1	NA	NA	NA	0.0142	0.5	0.0142
141	1.021	0.069	0.09	0.0331	0.12	NA	NA	NA	0.0142	0.5	0.0142
142	1.018	0.082	0.1	0.0428	0.13	NA	NA	NA	0.0142	0.5	0.0142
143	1.008	0.092	0.1	0.0512	0.17	NA	NA	NA	0.0142	0.5	0.0142
144	1	0.1	0.1	0.0578	0.18	NA	NA	NA	0.0142	0.5	0.0142
145	0.982	0.108	0.09	0.065	0.2	NA	NA	NA	0.0142	0.5	0.0091
146	1.046	0.054	0.1	0.0229	0.1	NA	NA	NA	0.0091	0.5	0.0091
147	1.037	0.063	0.1	0.029	0.12	NA	NA	NA	0.0091	0.5	0.0091
148	1.047	0.083	0.13	0.044	0.16	NA	NA	NA	0.0091	0.5	0.0091
149	1.025	0.095	0.12	0.0536	0.18	NA	NA	NA	0.0091	0.5	0.0091
150	0.987	0.103	0.09	0.0607	0.22	NA	NA	NA	0.0091	0.5	0.0091
151	0.09	0.035	0.03	0.0073	0.09	0.19	NA	NA	0.002	0.3	0.002
152	0.09	0.038	0.065	0.0087	0.082	0.19	NA	NA	0.002	0.3	0.002
153	0.09	0.047	0.08	0.0091	0.06	0.17	NA	NA	0.002	0.3	0.002
154	0.09	0.039	0.057	0.0097	0.096	0.2	NA	NA	0.002	0.3	0.002
155	0.09	0.043	0.073	0.0106	0.093	0.2	NA	NA	0.002	0.3	0.002
156	0.09	0.046	0.034	0.0113	0.125	0.25	NA	NA	0.002	0.3	0.002
157	0.09	0.053	0.072	0.0135	0.115	0.24	NA	NA	0.002	0.3	0.002
158	0.09	0.056	0.085	0.0147	0.098	0.21	NA	NA	0.002	0.3	0.002
159	0.09	0.056	0.067	0.0148	0.126	0.23	NA	NA	0.002	0.3	0.002
160	0.09	0.056	0.077	0.0148	0.0109	0.21	NA	NA	0.002	0.3	0.002
161	0.09	0.021	0.025	0.0045	0.035	0.38	NA	NA	0.002	0.3	0.002
162	0.09	0.033	0.03	0.0087	0.088	0.54	NA	NA	0.002	0.3	0.002
163	0.09	0.035	0.081	0.0098	0.05	0.43	NA	NA	0.002	0.3	0.002
164	0.09	0.039	0.034	0.0109	0.105	0.56	NA	NA	0.002	0.3	0.002
165	0.09	0.04	0.061	0.0117	0.075	0.47	NA	NA	0.002	0.3	0.002
166	0.09	0.044	0.035	0.0129	0.137	0.67	NA	NA	0.002	0.3	0.002
167	0.09	0.043	0.086	0.0136	0.062	0.46	NA	NA	0.002	0.3	0.002
168	0.09	0.047	0.079	0.0141	0.086	0.47	NA	NA	0.002	0.3	0.002
169	0.09	0.047	0.062	0.0144	0.145	0.59	NA	NA	0.002	0.3	0.002
170	1	0.368	0.531	0.379	0.45	NA	NA	NA	0.06	10.5	0.06
171	0.82	0.368	0.511	0.379	0.65	NA	NA	NA	0.06	10.5	0.06
172	0.6	0.368	0.482	0.379	0.5	NA	NA	NA	0.06	10.5	0.06
173	1.3	0.46	0.669	0.531	0.55	NA	NA	NA	0.06	7.5	0.06
174	0.9	0.46	0.624	0.531	0.65	NA	NA	NA	0.06	7.5	0.06
175	0.6	0.46	0.578	0.531	0.65	NA	NA	NA	0.06	7.5	0.06
176	0.55	0.46	0.568	0.531	0.65	NA	NA	NA	0.06	7.5	0.06
177	1	0.372	0.536	0.386	0.35	NA	NA	NA	0.06	10.3	0.06
178	0.65	0.38	0.502	0.398	0.45	NA	NA	NA	0.06	10	0.06
179	1.2	0.405	0.594	0.437	0.35	NA	NA	NA	0.06	9.1	0.06
180	0.68	0.368	0.493	0.379	0.4	NA	NA	NA	0.06	10.5	0.06
181	1.35	0.365	0.559	0.375	0.25	NA	NA	NA	0.06	10.6	0.06
182	0.72	0.361	0.491	0.369	0.15	NA	NA	NA	0.06	10.8	0.06
183	6	1.493	2.32	3.1	1.3	NA	NA	NA	0.051	18.7	0.051
184	0.3	2.292	1.859	5.9	0.7	NA	NA	NA	0.032	9.3	0.032
185	1.6	2.025	2.311	4.9	1.4	NA	NA	NA	0.039	11.2	0.039
186	2.5	1.525	1.999	3.2	0.8	NA	NA	NA	0.029	12.5	0.029
187	0.9	2.445	2.413	6.5	1.2	NA	NA	NA	0.035	9.8	0.035
188	2.8	2.08	2.627	5.1	1.3	NA	NA	NA	0.046	14.6	0.046
189	5.5	2.08	2.986	5.1	1.7	NA	NA	NA	0.032	16.1	0.032
190	2.5	2.025	2.516	4.9	2	NA	NA	NA	0.025	16.5	0.025
191	1.8	1.679	2.031	3.7	0.5	NA	NA	NA	0.034	3.3	0.034
192	1.3	2.134	2.318	5.3	1.1	NA	NA	NA	0.05	18.2	0.05
193	2.8	2.053	2.599	5	1.5	NA	NA	NA	0.048	11.8	0.048
194	5.3	3.961	4.996	13.4	1.4	NA	NA	NA	0.031	5.4	0.031
195	2.3	1.258	1.684	2.4	0.4	NA	NA	NA	0.071	8	0.071
196	2.8	1.395	1.9	2.8	0.5	NA	NA	NA	0.057	7.5	0.057
197	1	1.361	1.532	2.7	0.9	NA	NA	NA	0.053	8	0.058
198	2.6	1.188	1.645	2.2	1.3	NA	NA	NA	0.066	9.8	0.066
199	2.5	1.395	1.86	2.8	1.4	NA	NA	NA	0.042	8	0.042
200	2.8	1.46	1.972	3	0.4	NA	NA	NA	0.051	7.4	0.051
201	5	2.42	3.315	6.4	1.9	NA	NA	NA	0.053	9	0.053
202	3.8	1.885	2.57	4.4	1.8	NA	NA	NA	0.093	13.8	0.093
203	3.8	1.293	1.894	2.5	1.3	NA	NA	NA	0.1	12.5	0.1
204	2	0.793	1.128	1.2	1.1	NA	NA	NA	0.058	5.5	0.058
205	6.2	2.369	3.395	6.2	1.3	NA	NA	NA	0.064	17.5	0.064
206	5.2	2.369	3.283	6.2	1.6	NA	NA	NA	0.019	17.6	0.019
207	4.8	2.24	3.09	5.7	2.5	NA	NA	NA	0.073	25	0.073

(continued)

Appendix 1. Continued

Number	Z(m)	Ho(m)	H(m)	Q/B	s(m)	xs	hd	XD	d ₅₀	B	d ₉₀
208	4	2.618	3.386	7.2	2	NA	NA	NA	0.075	20	0.075
209	2.8	2.947	3.483	8.6	2.4	NA	NA	NA	0.078	18.5	0.078
210	4	2.97	3.751	8.7	3.5	NA	NA	NA	0.067	21	0.067
211	0.018	0.05	0.048	0.0185	0.032	NA	NA	NA	0.0085	0.6	0.0085
212	0.024	0.05	0.055	0.0208	0.042	NA	NA	NA	0.0085	0.6	0.0085
213	0.037	0.06	0.064	0.0238	0.045	NA	NA	NA	0.0085	0.6	0.0085
214	0.049	0.06	0.073	0.0275	0.046	NA	NA	NA	0.0085	0.6	0.0085
215	0.056	0.07	0.077	0.0292	0.05	NA	NA	NA	0.0085	0.6	0.0085
216	0.019	0.03	0.03	0.0073	0.016	NA	NA	NA	0.0085	0.6	0.0085
217	0.028	0.04	0.043	0.0125	0.036	NA	NA	NA	0.0085	0.6	0.0085
218	0.04	0.05	0.053	0.163	0.035	NA	NA	NA	0.0085	0.6	0.0085
219	0.059	0.05	0.065	0.0208	0.047	NA	NA	NA	0.0085	0.6	0.0085
220	0.069	0.06	0.072	0.0238	0.053	NA	NA	NA	0.0085	0.6	0.0085
221	0.046	0.02	0.033	0.0067	0.025	NA	NA	NA	0.0085	0.6	0.0085
222	0.061	0.03	0.044	0.01	0.034	NA	NA	NA	0.0085	0.6	0.0085
223	0.083	0.04	0.058	0.15	0.05	NA	NA	NA	0.0085	0.6	0.0085
224	12.9	2	5	4.571	3	NA	NA	NA	0.1	25	0.0085
225	57	29.69	40	275	28	NA	NA	NA	2.1	58	0.0085
226	19.2	6.85	7	38.97	6.2	NA	NA	NA	0.75	11.6	0.0085